Towards the Atomic Scale Simulation of Intricate Acidic Aluminosilicate Catalysts

Céline Chizallet

Towards the Atomic Scale Simulation of Intricate Acidic Aluminosilicate Catalysts

*Céline Chizallet**

IFP Energies nouvelles – Rond-Point de l'Echangeur de Solaize – BP 3 69360 Solaize, France

celine.chizallet@ifpen.fr

KEYWORDS. Zeolite, dealumination, external surface, amorphous silica-alumina, Brønsted acid sites, Lewis acid sites, Density Functional Theory.

ABSTRACT. Zeolites are nanoporous aluminosilicates with well-defined crystalline structures, considered key assets in heterogeneous catalysis, with a broad range of industrial applications. Computational investigations dealing with zeolite catalysts have been undertaken for decades with simple models of the bulk sites, known to be bridging Si_{IV}-OH-Al_{IV} groups, in the case where the compensation cation is a proton. Real zeolite catalysts used in practice are however finite size and intricate objects, with external surface sites and defects, among other sources of complexity. Amorphous Silica-Alumina may also be obtained as a consequence of zeolite post-treatments, or synthesized on purpose to obtain acid sites that are milder than those of zeolites. In the present Perspective, some of the achievements in the field of the atomic-scale simulation of intricate aluminosilicate catalysts (zeolites, amorphous silica-aluminas) of industrial relevance are reviewed. Emphasis is put on the simulation of the mechanisms of post-treatments of zeolites, and on the special structure and reactivity of acid sites at external surfaces of zeolites and on amorphous silica-alumina, that is shown to differ from the properties of the bulk bridging sites. Moreover, directions for future investigations are proposed.

1. INTRODUCTION AND OPEN QUESTIONS

The tailoring of highly selective catalysts is a major issue in chemical reactivity. Zeolites are key-players in that respect. They are nanoporous (historically called "microporous", pore diameter lower than 2 nm) aluminosilicates with a well-defined crystalline structure.[1-2] They can be described as a three-dimensional network of TO_4 tetrahedra (where T is mostly Si). These tetrahedra are linked at their corner via a common oxygen atom to form a secondary building unit (SBU). More than 230 zeolite structures (natural and synthetic) have been identified and listed on the International Zeolite Association (IZA) website.[3] Often, the synthesis is oriented by the choice of a Structural Directing Agent (SDA). The presence of Al^{3+} cations in crystallographic positions otherwise occupied by Si^{4+} is compensated in terms of charge by extra-framework cations, conferring zeolite a large array of properties such as ion exchange, gas separation and catalysis.[4-5] In particular, zeolites are widely employed as catalysts in industrial-scale refining and petrochemical processes due to their particular properties such as high adsorption capacity, hydrothermal stability, shape selectivity, Brønsted and Lewis acidity.[6-8] They are also used in pollution abatement,[9-11] and are promising candidates for biomass conversion.[12-15]

Their well-defined crystalline structure together with the large diversity of pore architectures, make that the relationship between the structure and acidity of the bulk sites was studied extensively for some decades.[16-22] The nanoporosity itself is also at the origin of peculiar interactions with reactants, products or transition structures by confinement effect,[23-24] at the origin of the so-called shape selectivity.[25-27] These made possible the design of catalysts from structural considerations, in particular for CO_2 capture,[28] for the production[29] or transformation of hydrocarbons[30-31] and of biomass derivates.[13]

Moreover, if a proton is the compensation cation, a case that I will consider further in this Perspective, it is known for decades that bridging Si_{IV}-OH-Al_{IV} hydroxyls, where silicon

and aluminium are both in tetrahedral coordination, are the Brønsted acid sites in the nanoporosity (Figure 1-a).[32-34]

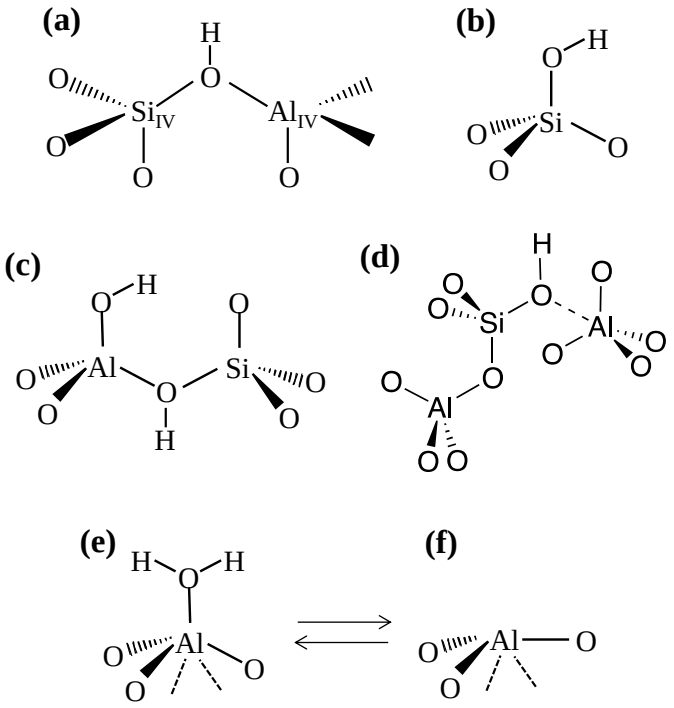

Figure 1. Some of the possible hydroxyl groups present in and on intricate protonic aluminosilicate catalysts: (a) bridging Si_{IV}-(OH)-Al_{IV} groups, (b) silanols at the external surface and at defects, (c) Al-OH groups close to bridging OH groups at the external surface of zeolites, discussed in ref. [35-39], (d) Pseudo-Bridging Silanols (PBS) suggested by *ab initio* calculations on amorphous silica-alumina,[40-41] represented as confirmed by NMR,[42] (e) water molecules adsorbed at surface aluminium, suggested by *ab initio* calculations at the external surface of zeolites,[38-39] and on amorphous silica-alumina,[40] the coordination number of aluminum may vary from IV to VI depending on the location at the surface, the temperature and the water partial pressure. (f) Lewis acid sites at the external surface of zeolites and on ASA, suggested by ab initio calculations, obtained upon dehydration of (e).[38-41]

Knowing this, it is possible to build a model of the interior of the perfect crystalline system. This explains why computational investigations dealing with the bulk of zeolites have been undertaken for decades:[16-17,20] a short section will be devoted to such simulations in this Perspective (section 3). However, the behaviour of real zeolite catalysts will not be quantitatively anticipated, as long as we restrict our understanding to the ideal nanopore sites. Indeed real zeolite catalysts are much more intricate than the simplistic picture of bridging OH groups all equivalently distributed in nanopores.

First, zeolite crystals are finite size objects, that exhibit an external surface (by contrast with the internal surface, in nanopores). Big zeolite particles (several μm, figure 2-a) are used at the laboratory scale to better understand the structure and reactivity of the inner parts of the crystals,[43-44] but zeolite particles that are used in practice exhibit much smaller crystal sizes, so as to shorten the diffusion path of reactants and products. Crystallites of much reduced size are more and more looked at, such as nanocrystals (below 100 nm, Figure 2-b),[45-46] embryonic zeolites (below 10 nm, Figure 2-c), [47-48] zeolite nanosheets[49] (Figure 2-d), nanoslabs,[50] delaminated and 2D zeolites.[51-52] From infra-red, the presence of silanols (Figure 1-b) at the external surface is known,[53] but their weak Brønsted acidity cannot account for the observation of pore-mouth catalysis,[54-55] when reactants that are too bulky to enter the pore are nevertheless converted by acid-catalysis.

Second, zeolite crystals exhibit a variety of poorly-defined defects. This is due to difficulties that may arise in crystallization control in the synthesis medium, or to post-treatments with steam or aqueous solutions. These are applied on purpose to zeolite crystals to increase the Si/Al ratio (thus, to tune the number of acid sites) and to generate mesopores (diameter > 2 nm, Figure 2-e), again in the aim to decrease diffusion limitations.[56-60] Dealumination is usually performed by steaming or acid leaching, whereas desilication is done by basic leaching.[6,58,61] These methods not only generate point or extended defects such as mesopores, but also extra-framework species, dislodged from their framework position but not eliminated in the post-treatments, in particular EFAl (Extra-framework aluminium). The mechanisms at the atomic scale of the dealumination/desilication reactions (that imply the hydrolysis of Si-O-Si and Si-O-Al bridges), the preference for the dealumination/desilication of certain T sites and zeolites, the way the defects propagate in the framework,[62] with a subtle interplay between thermal effects and water-induced mobility of cations,[63-64] are however poorly known, despite decades of research.[58]

Moreover, some amorphous zones can exist after synthesis and/or post-treatment of zeolites, with specific Brønsted acidity. Amorphous silica-alumina (ASA) is indeed suspected as debris in (non-leached) dealuminated zeolites,[65-70] whereas ASAs in general are reputed for their milder acidity as compared to zeolites.[71] Due to their amorphous nature, these solids are by far less understood that crystalline zeolites, and there is still a debate on the nature of the Brønsted acid sites on ASA. Some authors claim that they are bridging Si-(OH)-Al groups,[72-75] i.e. same as in zeolites, while others propose alternative structures to explain the absence of bridging OH group signature in the infra-red and ^{1}H NMR spectrum of some ASA samples.[76-90] Such question is related to the nature of the acid sites of the amorphous embryonic zeolites, which is not known to date.[48,91]

Finally, in industrial reactors, all aluminosilicate catalysts are shaped with binders (typically, alumina, silica, or other kinds of aluminosilicates) and other additives, so as to produce millimetre-sized objects such as extrudates or spheres (Figure 2-f). [92-94] Their impact on the zeolite's properties (structure, acidity) is poorly understood,[92] despite very recent experimental work, including advanced characterization techniques.[93,95-99] Shaping induces physical and chemical modification of the zeolites, and thus affects their catalytic performance.[95,97,99-102] The atomic-scale level of knowledge of these modifications is strongly limited.

Quantum chemistry, in particular density functional theory (DFT) calculations, have proven to be highly relevant to elucidate the nature of active sites and mechanisms of reactions taking place at the bulk bridging OH groups of zeolites.[16-17,20-22,103-107] The various sources of complexity above mentioned now need to be taken into account in the simulations. Notably, the question of how to take into account complexity in the simulation of heterogeneous catalysis is not restricted to the case of aluminosilicates.[108-110] After briefly setting the scene in terms of relevant methodologies (section 2) and a short overview of the state-of-the-art with respect to the simulation of bulk sites (section 3), the present Perspective

reports recent achievements in the field of first principles approaches of the complexity of intricate aluminosilicate catalysts. First, the simulation of defect formation upon zeolite post-treatments is addressed (section 4), then the specificity of the acid sites present at the external surface of zeolites (section 5), finally the structure and reactivity of amorphous silica-alumina (section 6). Future directions to reach an ever more realistic description of the systems are then proposed (section 7), keeping as a ultimate goal the prediction of the behavior of industrial-like catalysts.

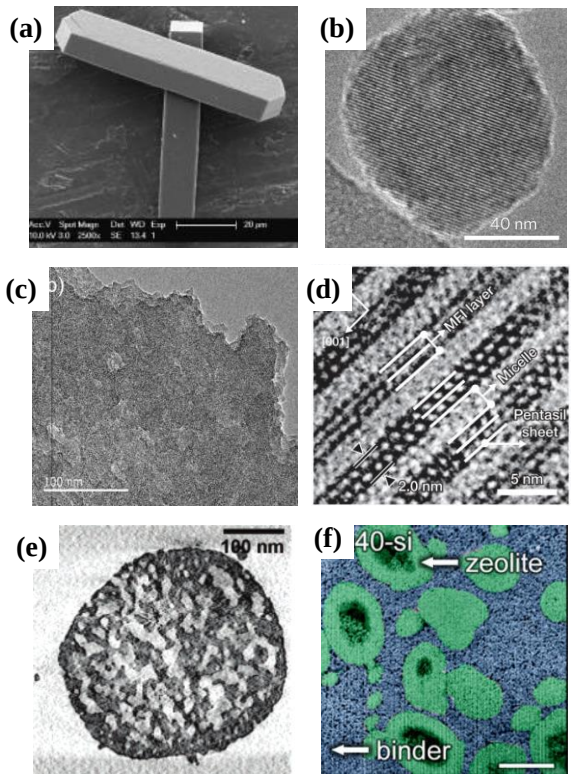

Figure 2. Scanning (a and f) and Transmission (b to e) Electron Microscopy pictures of zeolites, with MFI framework, at various sizes and hierarchical degrees (the scale bar is given in parentheses): (a) ZSM-5 coffin-shaped crystals (20 μm). Reproduced with permission from ref. [43]. Copyright 2008, American Chemical Society. (b) W-MFI defect-free nanocrystals (40 nm). Reproduced with permission from ref.[46]. Copyright 2017, Nature. (c) aggregated ensemble of ZSM-5 embryos (100 nm). Reproduced with permission from ref. [48]. Copyright 2018, American Chemical Society. (d) ZSM-5 nanosheets (5 nm). Reproduced with permission from ref.[49]. Copyright 2009, Nature. (e) micro-mesoporous hierarchical desilicated ZSM-5 (100 nm). Reproduced with permission from ref.[111]. Copyright 2005, American Chemical Society. (f) FIB-prepared cross-section of an extrudate of H-ZSM-5 shaped with silica (2 μm). Reproduced with permission from ref.[97]. Copyright 2014, American Chemical Society.

2. A FEW METHODOLOGICAL CONSIDERATIONS

2.1. Calculation of the energy of the system, and of derived quantities

Our aim is to model atomic ensembles and their interactions, in the course of chemical reactions. A first and efficient technique consists in using analytical potentials for this, called forcefields, then considering that atoms interact according to Newton's mechanics. This approach, called molecular mechanics (MM), has been extensively used for the simulation of adsorption isotherm and diffusion of various molecules in zeolite frameworks, as well as for template design.[20,24,112] For catalytic materials and reactions, most of the time, such an approach is however not sufficient, because we are dealing with variable coordination for surface species, due to dangling bonds at the surface and the existence of defects, and due to the catalytic reaction itself. In such cases, quantum chemistry needs to be considered. The goal of these calculations is to solve the Schrödinger equation $H\Psi = \varepsilon\Psi$, which can only be done approximately for polyelectronic systems. Two philosophies can then be chosen: one may chose specific mathematical expressions for the wavefunction Ψ, keeping an exact expression of the Hamiltonian H, or at reverse choose approximate expressions of H. The wavefunction methods correspond to the first philosophy, whereas DFT, in practice, obeys the second one. The exchange-correlation functional gathers all the tricky terms of DFT, its choice impacts both the accuracy and cost of the calculation.[107-108] Long-range interactions have been shown to be crucial for reactions in zeolites,[107] in particular electrostatic and van der Waals interactions. Due to its significant computational cost, quantum approaches are however limited in terms of size of the simulations (number of atoms, number of steps), and of accuracy. A compromise between the level of realism, the accuracy and the calculation cost is always required.

Obtaining the optimal geometry of systems corresponding to local energy minima requires the minimization of forces, which is called a geometry optimization. With dedicated algorithms, transition structures can also be determined. This ensemble of methods is called

the static approach. Indeed, the effect of thermal motions is not explicitly addressed in such calculations, and the reactant, the product, the intermediates and transition states are defined by a single structure each. Once these structures are known, their electronic and spectroscopic properties can be determined thanks to the analysis of the electron density and shape of the neighboring potential energy surface. In particular, the vibrational degrees of freedom may be determined, giving rise to an estimation of the vibration partition function, and of the corresponding free energy. Free energy profiles along a reaction path are thus calculated. As will be shown in section 3, in some cases, this approach appeared to be unsatisfactory for the identification of reaction intermediates in acid-catalyzed reactions in zeolites, and for the accurate quantification of their free energy.

A costly alternative is ab initio molecular dynamics (AIMD), which consists in the calculation of the propagation of the movement of the considered particles, by the integration of the Newton's equations (often, the nuclei are treated classically), according to a given time step. The quality of the result depends on the level of theory used for the calculation of forces and on the length of the trajectory, itself limited by calculation time. Reaction events are rare with respect to non-reactive thermal motions, so that quantification of free energy profiles requires to bias the system, for example by forcing it to follow the direction given by a chosen reaction coordinate. Several approaches (metadynamics, umbrella sampling, bluemoon sampling, transition path sampling, etc.) have been applied in the case of zeolite science with success,[104,113-124] but can currently not be considered as routine techniques, both due to limitation in computational time, and to difficulties in defining relevant variable coordinates.

2.2. Structural models

A model of the catalytic site needs to be constructed. Contrary to organic molecules or small organometallic complexes, a single zeolite nanocrystallite already contains several thousands of atoms, which cannot easily lead to an explicit quantum calculation. Several

strategies can be chosen to overcome this problem, they are depicted in Figure 3 in the case of the simulation of a Brønsted acid site of a zeolite or ASA.

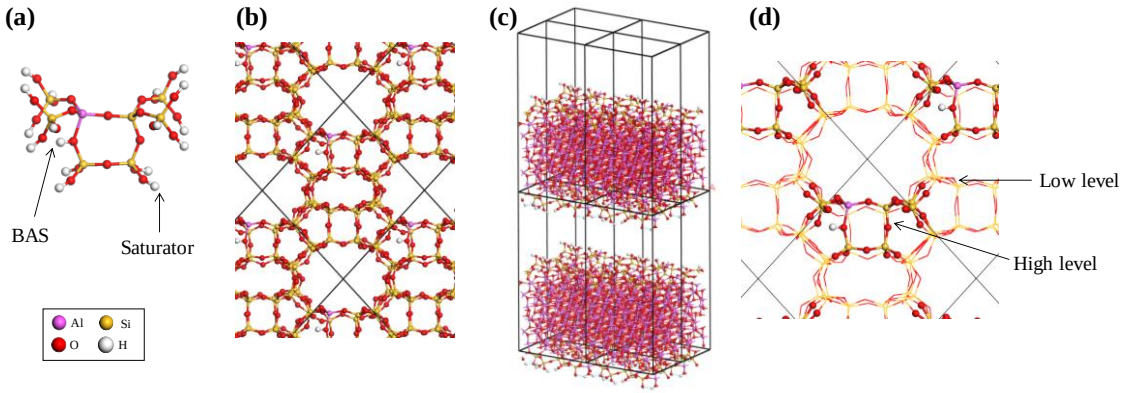

Figure 3. Various formalisms for the simulation of actives sites of a protonic zeolite, mordenite – MOR-, and an Amorphous Silica-Alumina surface: (a) cluster containing 8 T sites (Al and Si), the Brønsted acid site (BAS) is shown, all other hydrogen atoms are saturators to remove dangling bonds; (b) periodic model of MOR, the unit cell is depicted by black lines; (c) periodic model of ASA, including a vacuum layer to obtain a surface model; (d) hybrid approach for the BAS of mordenite, two levels being considered, for the specific case of a periodic treatment of the low level part. For the sake of clarity, the saturating H are not depicted around the cluster chosen for the high level part.

The cluster approach (Figure 3-(a)) consists in the simulation of a fragment of a particle (expected to represent the active site) from 10 to several tens of atoms. The main advantage is that the system can be treated as a molecule, which is possible in many codes, with a large variety of alternatives for the level of the resolution of the Schrödinger equation, including state-of-the-art methods. Clusters were used right from the 70's to simulate aluminosilicates.[16-17,34,125-128] Portions of the structure have to be cut, which induces spurious electronic density variations at the border of the cluster. To remove these dangling bonds, the border of the cluster is usually saturated by H atoms. These atoms are however at the origin of deviations of electronic properties from that of the full solid. Moreover, taking into account the topology around the active site requires a significant number of T atoms (Al and Si), which renders the calculation quite demanding. Two strategies can be chosen to overcome the question of the accurate simulation of long range effects.

The periodic approach consists in the simulation of an elementary cell, containing from several tens to several hundreds of atoms. The cell is periodically replicated over three directions in space for the simulation of a crystal (Figure 3-(b)). For the simulation of an infinite surface, a vacuum layer is introduced in the cell (Figure 3-(c)). In this last case, the layers representing the solid are called a "slab". This approach has become highly popular since the 90's for the first principles simulation of zeolites,[20,103,129-132] as the crystallographic structure of the latter is known, thus the initial content of the cell can be rather easily defined.

Another strategy considers the cluster as a first level, and tries to make it a better model for the heterogeneous catalyst. In the spirit of hybrid schemes developed for the simulation of macromolecules by Warshel, Levitt and Karplus (the Nobel Prizes in Chemistry 2014), in particular biomacromolecules,[133-135] embedding species can be added in the surrounding of the cluster to describe, at a lower level of theory, the remaining part of the catalyst particle.[107,136-138] The "low level" part can be treated either periodically (Figure 3-(d)) or as a macromolecule, with force-fields or at a "low" quantum level. The "high level" part is the cluster investigated with much more accurate first principles approaches. When the "low level" part is addressed with molecular mechanics (MM), and the "high level" part with quantum chemistry (QM), this approach is called QM/MM.

Whatever the approach chosen, simulating defects or surface sites, or accounting for the amorphous nature of ASA, requires the construction of much bigger systems (larger cells for periodic simulations) than for bulk sites, due to loss of symmetry. This explains why such simulations have been rather poorly undertaken in the past. The evolution of high performance supercomputing is key in progressing in that field.[139]

Should the reactions investigated take place in a solvent, the simulation of its effect is required. This shall be done either considering the solvent molecules explicitly –most of the time performing molecular dynamics, or implicitly. In this last case, the solvent is represented as a continuum, with electrostatic models of the solvent/solute interactions. [140] This prevents

the accounting of effects linked to hydrogen bonding. Hybrid QM/MM approaches may also be chosen.[141]

3. PRELIMINARY: COMPUTATIONAL INVESTIGATIONS OF BULK BRIDGING OH GROUPS

The corpus of computational studies of the properties of bulk protonic zeolites is huge, reviewing all of it is beyond the scope of the present Perspective. The reader is referred to previous reviews that directly or indirectly deal with this.[16-17,20-22,103-107] Important questions that are still vivid in this field, and that also apply when dealing with defects, are listed below.

3.1. Where is the acid site ?

To start a calculation, one needs to locate aluminum atoms is specific T sites locations, as well as the associated proton. However, these locations (in terms of bulk crystallographic position) remain largely unknown for most frameworks. In practice it depends on synthesis conditions,[142-146] but due to the very close atomic weights of Si and Al, the Al sitting cannot be deduced from X-Ray Diffraction. X-Ray standing waves fluorescence appeared to be a promising technique in that respect, but appeared to be limited to a very small number of frameworks.[147] Multiquantum ^{27}Al NMR experiments give some insights (in particular for MFI,[142,146,148-150] FER,[151-152] BEA*,[153-155] CHA[156] frameworks).

The intrinsic stability of all occupation configurations was exhaustive sampled for several frameworks (by DFT or forcefield approaches).[35,38-39,157-169] Typically, the stability varies by at most 50-60 kJ/mol. Not all studies agree on the preferred location of the {Al,H} pairs, suggesting that the difference in stability of these sites is not pronounced enough to draw conclusions, and that kinetic factors may also play an important role. Thus, in the absence of clear preference of Al for a given T site, for DFT calculations, sampling several (if not all) possible sites is needed.[159,170] Also, the number of Al to be considered per simulation

unit cell needs to be addressed, to investigate the effect of the Si/Al ratio, having a crucial impact both on post-treatment mechanisms, and on the acidic properties.

Notably, the mobility of the protons inside the framework, activated by high temperatures and by the presence of water as carrying agent,[171] makes the comparison between calculations and experiments a challenge at finite temperature.[172] Molecular dynamics provide useful information about this process.[171,173-174] In that respect, nuclear quantum effects are expected to play a role, [175-176] and should in principle be taken into account for a proper quantifications of the properties of mobile protons in zeolites. Developments relying on Path Integral MD (where the nuclei are now treated quantum mechanically) make this feasible,[177-178] but to the best of my knowledge, no report of an application of these methods to the case of protonic zeolites was ever published so far.

3.2. Quantification of the acidity of bulk bridging OH groups

Several earlier cluster investigations consisted in the quantification of the intrinsic acidity of bridging OH groups through their deprotonation energy,[17,34,179] or proton affinity of the conjugated base.[180-182] Correlations with T-O-T angles were invoked on the basis of semi-empirical calculations,[182] but not found any more in more recent Hartree-Fock[183] and DFT[184-185] investigations. The transposition of such approaches to periodic calculations raises the problem of the electroneutrality of the cell, generally compensated after proton removal by a positive background charge.[183] This makes the comparison of the deprotonation energy for several sites of a given site possible, but not truly relevant from one kind of cell to another.[185] Recently, Sauer et al. proposed the decomposition of the deprotonation energy into an intrinsic deprotonation energy and a proton "solvation" energy (dependent on the dielectric constant of the material), that they estimate thanks to a QM/MM approach.[184]

Mimicking the experimental procedure consisting in the adsorption/desorption of basic probe molecules susceptible to interact with Brønsted acid sites,[53,186] many computational

works (that cannot be cited exhaustively here) have been devoted to the simulation of the adsorption of molecules such as carbon monoxide, pyridines, amines, to name a few. The quantification of acidity using such calculations differs from that of the deprotonation energy: not only the intrinsic acidity of the site plays a role, but also the stabilization of the adsorbed molecule (or its conjugated acid, when proton transfer occurs) within the cavity, in particular when taking into account dispersion forces accurately.[16-17,103,107,187]

3.3. Reactivity investigations

Driven by the historical use of acidic zeolites in refining, petrochemistry, and natural gas conversion, a large majority of computational studies devoted to the reactivity of protonic zeolites deal with the transformation of various kinds of hydrocarbons, such as alkanes, alkenes, and aromatic.[17,20,104] An important question behind this is the impact of the level of theory and of the investigation method (static *versus* molecular dynamics) on the computed stabilities of possible reaction intermediates. Already, the nature of adsorption adducts and heats have been the objects of many improvements over the past decades. The impact of dispersion forces appeared to be key for the accurate description of the adsorption of alkanes,[188] as well as the accounting for anharmonicity corrections for the calculation of adsorption Gibbs free energies.[189]

In the case of alkenes, there have been a long debate about the prefered adsorption mode before (π-complex) or after protonation, with two competitive forms in the second case: carbenium ions *versus* alkoxides (see later Figure 8). For a long time, carbenium ions were claimed to be transition structures, alkoxides to be intermediates, on the basis of calculations performed on small clusters.[190-193] It then appeared that these conclusions were dependent on the structural models chosen for zeolites (small clusters *versus* bigger clusters, *versus* periodic boundary conditions), on the level of theory (Hartree-Fock, DFT versus post-HF methods) and on the simulation approach chosen (static *versus* AIMD).[104,116-117,121-122,194-199] Now,

carbenium ions are found to be reaction intermediates, in particular tertiary carbenium,[116,120-122,198] the situation being strongly temperature-dependant for secondary carbenium ions.[116,121-122] Beyond adsorption and protonation, much efforts were devoted to the elucidation of free energy profiles for reactions undergone by hydrocarbons, such as cracking, isomerization, alkylation, to name a few. Most recent investigations point out the need for dispersion corrections,[107,167] and either for AIMD,[104,116-118,120] or for high level of theory (beyond DFT, including anharmonicity corrections) for an accurate description of reaction intermediates and transition states.[200-203] The two kinds of requirements are currently hard to combine due to computational limitations.

Implementation of Brønsted acidic zeolite catalysis in fine chemistry and for biomass conversion motivates investigations of the reactivity of bulk bridging OH groups for the transformation of molecules containing oxygen atoms. I will put here a special emphasis on the question of the dehydration of alcohols, as a useful comparison with other acidic aluminosilicates will be done later (section 6.4.). Earliest published studies of methanol dehydration into dimethylether are suggesting the participation of alkoxides.[204-205] Depending on the investigated alcohols and sites, a debate still remains about the preferred mechanism (E2 *versus* E1) for water elimination in zeolites.[206-208] Significant effort was done by Reyniers et al. to determine the mechanisms and kinetic feature *ab initio* for 1-butanol dehydration into ethers and butenes in various zeolitic frameworks.[209-212] In particular they revealed the importance of a pathway implying ether decomposition for the formation of butene. They also built microkinetic models from these data, which consist in the integration of the rate equations for the whole set of elementary steps, using ab initio rate constants. This model reveals a strong dependence of the relevant intermediates and mechanisms on the operating conditions and catalyst's framework.

Thus, the knowledge obtained by computational methods about the structure, acidity and reactivity of bulk bridging OH groups in zeolites is more than significant, motivating ever

more numerous investigations combining experiments with theory. Some of the kinetic data quantified by these approaches start to be relevant enough to be close to chemical accuracy, opening the route for their integration in higher scale models, such as microkinetic schemes. This was attempted in a few cases so far for Brønsted acid catalysis by zeolites.[209,211-215] This approach brings useful information about trends, but the comparison with experimental results remains rather qualitative to date in the case of zeolites. Besides the challenges linked to the calculation of a large set of kinetic data at a sufficient level of theory, one of the factors that may explain this discrepancy is the need for taking into account the role of defects in the catalytic performance.

4. SIMULATION OF DEFECTS AND POST-TREATMENT MECHANISMS OF ZEOLITES

4.1. Proposals for the structure of defects and extra-framework species

Earlier works were devoted to the simulation of possible structures for point defects and extra-framework species, in particular EFAls. Isolated $[Al(OH)_x(H_2O)_{n-x}]^{3-x}$ aluminum complexes were used as simplistic models for EFAls, in tetrahedral, pentahedral and octoahedral coordination.[216] The structure and stability of these complexes were shown to depend on the charge hold by the complex, linked to its deprotonation degree, but the change in coordination number was shown not to require large energies (calculated at the MP2 level). The first simulations of the interaction of EFALs ($Al(OH)_3(H_2O)_3$ and $Al(OH)_3(H_2O)$) with a hole-free zeolite framework, was made by Benco et al.[217] with a periodic representation of the gmelinite zeolite, and AIMD at 300 K. Two water molecules detached the octahedral aluminum atom in the course of the dynamics. The mobility of the EFAl appeared to be strongly dependent on the local topology, with possible immobilization in cages (Figure 4-a), that then become occluded, thanks to hydrogen-bonds. Proton transfer from bridging OH groups and neutral EFAls was observed, revealing the basic character of this neutral EFAl.

Bhering and co-workers[218] undertook a DFT simulation of the interaction of some EFAl (Al^{3+}, $Al(OH)_2^+$, $Al(OH)_3$) with faujasite, modeled as a T_6 cluster containing one bridging OH group. The structure and stability of the EFAl was shown to depend strongly on its hydration degree. Embedded cluster simulations combined to ^1H NMR experiments also confirmed that when considering a mononuclear octoahedral aluminum atom as an EFAl in faujasite, some of the water molecules connected to the aluminum atom can be qualified of mobile.[219]

Benco et al. also investigated the preferred location of the bare Al^{3+} ion as EFAl within a periodic Mordenite framework, formally considered as the compensation cation corresponding to three framework aluminum.[220] They observed limited relaxation of the framework around this EFAl. Most favorable configurations correspond to a connection of the Al^{3+} cation to oxygen atoms themselves connected to framework aluminum atoms. This EFAl exhibits strong Lewis acidity probed by CO. More recently, Pidko et al. published a series of periodic DFT works dealing with the possible structure of monomeric and multimeric (up to 4 aluminum atoms) EFAls in faujasite, the bigger species (3 and 4 Al) being stabilized in the sodalite cage. This induces acidity enhancement of neighboring bridging OH groups in the supercages,[221-222] assigned to the additional compensation of the negative charge of the deprotonated lattice sites by the multiply charged cationic EFAl cluster. This may be seen as an effect of the Si/Al_{total} ratio, if one includes in its estimation the EFAl content.

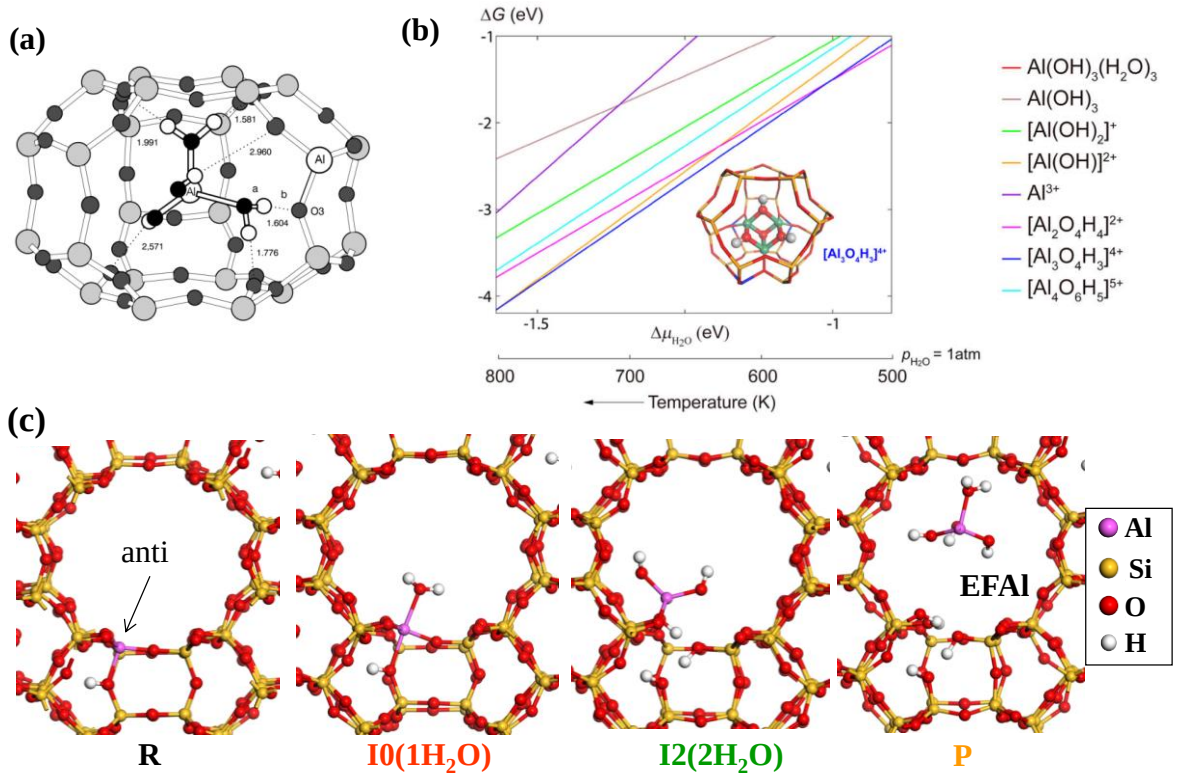

Figure 4. (a) $Al(OH)_3(H_2O)$ species occluded in the cage of gmelinite. The acidic proton of the bridging OH group is transferred to the hydroxyl group of the EFAL. Reproduced with permission from ref.[217]. Copyright 2002, Elsevier. (b) Calculated relative Gibbs free energies of EFAl species in faujasite zeolite as a function of water chemical potential. The most stable trimer is drawn. Reproduced with permission from ref. [221]. Copyright 2015, American Chemical Society. (c) Dealumination intermediates from the T4O4 site in mordenite. The names of the intermediates correspond to the number of water molecules added, and to the location of the free energy diagram of Figure 5-b. Redrawn form data published in ref. [223].

Such a synergy effect between Brønsted and Lewis acid sites of faujasite was invoked before from experimental observations,[224] and analyzed on (embedded) cluster models, with contradictory conclusions from one study to another. Computing deprotonation and ammonia adsorption energies, Mota et al.[225-226] found that the intrinsic Brønsted acidity of bridging OH groups is reduced upon proximity with an EFAl, but that the conjugated base is stabilized by hydrogen bonds thanks to the EFAl. Combining NMR and DFT, and using acetone as a probe molecule, Deng et al. observe an increase in Brønsted acidity of bridging OH groups even in the absence of these hydrogen bonds.[227] A specific role of tricoordinated aluminum atoms as EFAls was proposed,[228] this species exhibiting strong Lewis acidity with respect to trimethylphosphine. These diverse conclusions regarding the Brønsted/Lewis synergy suggest

a significant dependence of the phenomenon upon the structure and nucleation degree of the EFAl species, and on the modeling method employed for the simulation of their interaction with the framework.

However, the removal of framework hydroxylated Al or Si species, upon hydrolysis of Si-O-Si and Si-O-Al bridges, should also lead to the formation of a silanol nest, besides EFAl and EFSi (Extra-framework silicon) species. All the simulations mentioned above omit the effect of the presence of such species. A silanol nest is expected to be composed of four silanols surrounding the tetrahedral void.[229-231] Sokol et al. published a series of studies[232-235] dealing with the stability and reactivity of silanol nests and other kinds of non-stoechiometric defects in silicalite. All these species are considered to be possibly formed in the structure. Their lifetime is, however, strongly questioned.[236-237] As mesopores are formed, the propagation of the initial point defect may be invoked. Marcilly[6] proposed a tentative scheme consisting in the extraction of T sites connected to the first extracted one, and self-healing by EFAl and EFSi that would fill other holes, likely to explain the formation of mesopore without full dissolution of the solid. This is however only a tentative proposal, that deserves atomic-scale investigations.

4.2. Simulation of the dealumination / desilication mechanisms

Getting an accurate knowledge of the structure of defects however requires to know how these species are formed, as kinetic control prevails in zeolite chemistry. Most published computational work in that area deal with steaming post-treatments, meaning that gas phase water is considered as the reactant.

Possible intermediates in the formation of EFAl plus silanol nest, were first determined by Lisboa et al.,[238] using DFT on cluster models of H-ZSM-5. A full reaction pathway, including transition structures, for the formation of point defects and extra-framework species (EFAl - $Al(OH)_3H_2O$, or EFSi - $Si(OH)_4$) was first determined by Swang

et al.[239] starting from a H-SSZ-13 (CHA) periodic model (Figure 5-a). Dealumination was found to be a less activated process than desilication, when dealing with stepwise water attacks. The activation barriers, however, appeared to be prohibitive (close to 200 kJ/mol) due to a very unstable vicinal disilanol species, where two pentahedral silicon atoms are part of a two-membered ring. Similar disilanol intermediates were previously invoked as possible defects in siliceous zeolite models,[232-234] and were also invoked for the desilication of SAPO-34.[240]

Silaghi et al. identified much easier initiation steps for the dealumination mechanisms upon water attack,[223,241] leading to the formation of a $Al(OH)_3(H_2O)$ EFAl, and a silanol nest (Figure 5-b and 4-c). The most favorable orientation found for water attack is in anti with respect to the bulk bridging OH group. It is followed by a 1,2-dissociation of water on adjacent framework oxygen, leading to reasonable activation barriers (close to 100 kJ/mol), for CHA, MFI, MOR and FAU frameworks. A critical aspect orientating the regio-selectivity of the attack was shown to be the accessibility of the anti-position (rather than that of the bridging OH group itself). In H-ZSM-5, the sites located at the intersection between the straight and sinusoidal channels were shown to be the most prone to delalumination upon steaming, which was later confirmed experimentally.[146] DFT was used throughout these studies, which validity, in terms of energy of hydrolysis intermediate and transition states, was confirmed thanks to higher level calculations (MP2/DFT hybrid schemes).[241]

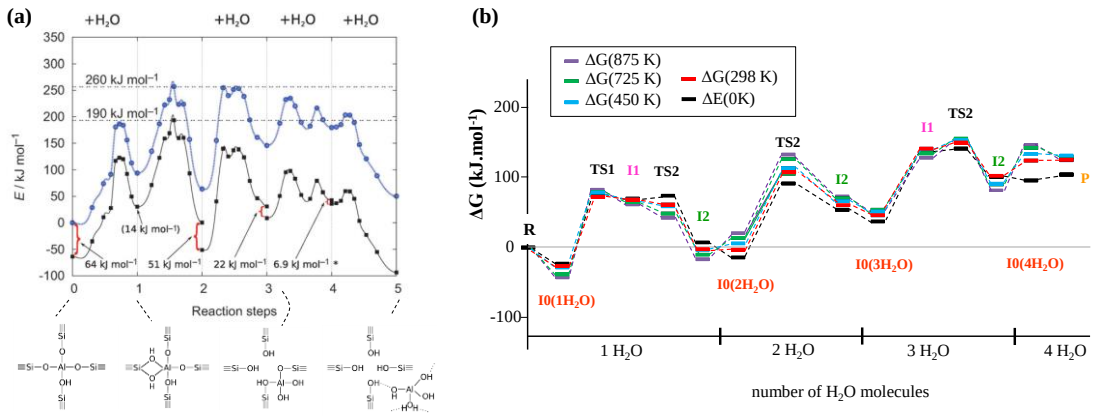

Figure 5. (a) Energy profile (top) and key-structures (bottom) for the dealumination mechanism of SSZ-13. The intermediate described at step 1 is called a vicinal disilanol. Reproduced with permission from ref. [239]. Copyright 2012, Wiley. (b) Free energy profile for the dealumination of the T4O4 site of mordenite, according to 1,2 dissociation with axial substitution elementary steps. Redrawn from data published in ref.[223]. Some of the intermediates are shown in Figure 4-(c).

Nielsen et al.[242] then published a detailed study where they predict the dealumination rate for SSZ-13 by kinetic modeling, as a function of temperature and water partial pressure, based on ab initio rate constants. The need was shown for considering the physisorbed state as a reference for water, rather than the gas phase state, based on the comparison of experimental and computed apparent Arrhenius activation energies. Similar mechanisms starting by water adsorption on aluminum were moreover shown to be valid in the presence of HCl,[243] and for the dealumination of zeolites exchanged with cations different than protons.[169,244-245] The anti-approach to silicon also appeared as relevant to infer Si-O-Si breaking mechanisms.[246]

The previously mentioned investigations usually consider a stepwise mechanism for the breaking of the Al-O-Si and Si-O-Si bonds, whereas several water molecules may play a role in a same elementary step.[247] Very recently, the cooperative role of water molecules for the dealumination and desilication pathways was taken into account (instead of adding molecules one by one) either in static (for MFI)[248] or AIMD simulations (for CHA).[119,246] These studies show that the anti-approach is still valid in these conditions, but barriers are made lower thanks to the cooperation. Alternative mechanisms also become possible when increasing the water loading,[248] or when considering already partially dislodged aluminum species,[223] suggesting that the complexity of the reaction landscape increases with the number of available directions for proton jumps. Very recently, the effect of the presence of a second inequivalent aluminum atom in the SSZ-13 cell (thus, of the Si/Al ratio) was analyzed by periodic static calculations.[169] It appeared that the water attack on the second Al becomes easier once the close Al is dislodged.

4.3.Outlooks

Most of the investigations reported in section 4.2 deal with the interaction of water with zeolite frameworks, in conditions that are susceptible to be representative of steaming post-treatments. Except a few preliminary computational investigations,[243] the effect of ions that are present in solution (such as the one used in acidic or alkaline aqueous conditions) have not been considered. This requires the accurate simulation of confined aqueous solutions, which remains a challenge as AIMD shall be needed. Moreover, although interatomic potential simulations of extended defects have been proposed,[249] mechanistic ab initio studies have so far been restricted to the extraction of the very first extra-framework species, the feature of the propagation of the defects are unknown at the atomic scale. The evolution of the extra-framework species, in terms of location, migration, aggregation, is also a fully open question. Reactive forcefield, that have only scarcely be used in the simulation of zeolites,[250-253] are an attractive possibility to reach these goals, but optimizing an accurate reactive forcefield remains challenging. Finally, as mentioned in section 4.1., the consequences of the presence of defects on acidic properties was investigated computationally in the spirit of the validation of the synergy concept between Brønsted and Lewis acid sites. It requires to be extended to the various species generated in the course and at the end of the defect formation mechanisms.

5. EXTERNAL SURFACE MODELS

5.1. Structure of external surface sites

Considering the finite size nature of zeolite crystallites, the behavior of the external surface needs to be known at the atomic scale. The first achievements in this field have been motivated by the identification of the structure of specific surface terminations for purely silicic zeolites, exhibiting silanol groups. The method generally employed is the cut of the bulk structure along given crystallographic planes, then saturation with OH groups: hydrogen atoms are added to monocoordinated O atoms and OH moieties saturate $Si_{III}/Si_{II}/Si_{I}$ atoms.

Most of the works reported below are periodic, even if a few cluster simulations were also undertaken.[37,254]

Forcefield and *ab initio* simulations of external surfaces of zeolites, nanosheets or 2D zeolites, have been undertaken for various frameworks: SOD,[255,256] EDI,[257] MOR,[35,258-260] CHA,[261] BEC,[262] BEA,[38] LTL,[249] LTA,[263-265] UTL and ITH,[266] FAU,[267] MFI,[36,37,39,162,184,254,268-271] inter alia. 2D zeolites grown on metallic substrates, composed of silicate bilayers without any Si-OH group at native state, have been the object of specific simulations.[272-275] Algorithms defining the most stable orientations that minimizes the number of cut bonds have recently been proposed.[276] From a thermodynamic point of view, taking thermal effects into account, these orientations indeed appear as the most stable.[39] Equilibrium morphologies can be deduced from the calculation of the surface (free) energies of the exposed Miller plans. Rather nice agreement with experiments were obtained for sodalite[255] (surface energies determined by Buckingham potentials, Figure 6-a) and silicalite-1[39] (surface free energies determined by DFT, Figure 6-b), although it is known that kinetic factors, tuned by synthesis conditions, drive morphology changes experimentally. In the case of silicalite-1, a Si_{33} precursor structure has been proposed from a set of experiments by Kirschhock *et al*.[277] The construction of surface models from this building block appeared to be similar with the one deduced from the cut of the bulk crystal for the (010) and (100) orientations, but not for the (101) orientation.[39] This results in longer coffin-like geometries (Figure 6-c) than with the models cut from the bulk (Figure 6-b).

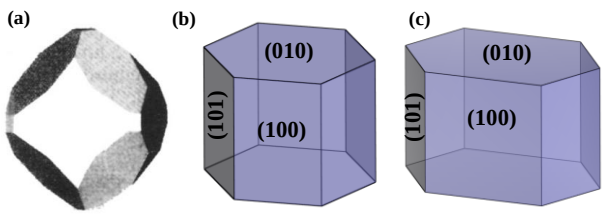

Figure 6. Calculated equilibrium morphologies of (a) sodalite, reproduced with permission from ref. [255]. Copyright 1994, Royal Society of Chemistry. (b)-(c) silicalite-1, reproduced with permission from ref. [39]. Copyright 2020, American Chemical Society. Surface models were obtained by cutting the bulk structure for (a) and (b), and deduced from a crystal growth approach for (c).

Brønsted acid sites can then be modelled starting from silicic slabs. The approach is similar as for the bulk (substitution of Si by {Al,H} pairs, section 3.1), but at the external surface part of the symmetry is broken due to the modified environment, which increases even further the number of configurations to be sampled. Several studies invoke bridging OH groups as the sole possible sites, mimicking the knowledge from perfect bulk sites, avoiding configurations that may lead to other types of sites, except Al-OH groups next to bridging OH groups (Figure 1-c).[35-37,162,184,254,261,271] Recently, we constructed external surface models for zeolite Beta[38] and ZSM-5,[39] that comprehensively model the location of compensation protons. According to these DFT calculations, bridging Si-(OH)-Al groups are still existing at the open nanopores (pores emerging at the external surface, Figure 7), giving a substance to the pore mouth catalysis concept.[54-55] However, at the outermost surface (no emerging nanopores), water molecules adsorbed on aluminum atoms (Al-$(H_2O)(OH)_n$ with n=0-2) prevail (Figures 1-e and 7). Notably, Al-(H_2O) was invoked before as an intermediate before dehydration.[36,258]

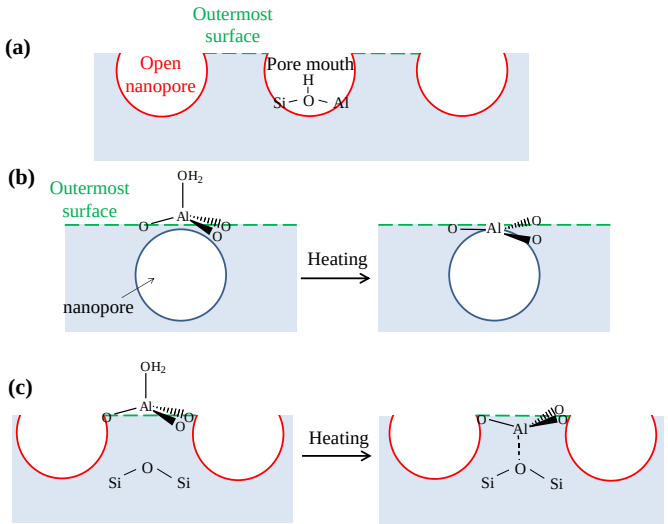

Figure 7. Dehydration of Al-$(H_2O)(OH)_n$ groups (exemplified in the case of n = 0) at the outermost surface of zeolites, according to DFT calculations, depending on the presence of a nanopore (b) or a siloxane bridge (c) below the Al atom, while bridging OH groups at the pore mouth (a) are stable upon dehydration. Adapted with permission from ref. [39]. Copyright 2020, American Chemical Society.

Indeed, the local structure of those surface Al atoms was shown to depend on the temperature and water partial pressure. Hydration (at low temperature, high water partial pressure, or in liquid water) is shown to lead to Al_V and Al_{VI} species, in agreement with experimental findings.[278-279] Dehydration was shown to proceed via condensation of silanols, giving birth to additional siloxane bridges, sometimes in the form of 2MR, and also via the desorption of water from Al-$(H_2O)(OH)_n$ species. Several situations were encountered on Beta and ZSM-5 (Figures 1-f and 7-b-c).[38-39] When a siloxane bridge is present close to the surface Al atom, water desorption is promoted by the formation of an additional Al-O bond with the oxygen of the siloxane bridge. However, if such bridge is not present close to the surface aluminum atom, desorption leads to a less stable surface Al_{III} atom. On mordenite[258] and ZSM-5,[36] some of the Al_{III} were shown to relax into a Si-Al 2MR ring upon bonding of a neighboring silanol group with the Al_{III}. This species was shown to be nearly of equal energy with respect to the separate silanol and Al_{III}.

5.2. Acidity of external surface sites

The diversity of surface groups revealed by DFT calculations at the external surface of zeolites suggests the possible expression of a diversity of acidity types (Brønsted, Lewis) and strengths. Computationally, this was probed by the quantification of the deprotonation energy,[162,184,261] and by the simulation of the adsorption of basic probe molecules such as CO,[38,271,280] pyridine,[39,260-261] ammonia,[259,261] 2,6-dimethylpyridine[261] and trimethylphosphine oxide.[281] The reactivity in terms of transfer ability to isobutene was also calculated in the case of zeolite Beta.[38] Generally speaking, bridging OH groups of the external surface maintain a similar acidity as that of the bulk, whereas Al-(H_2O) located at the outermost surface exhibit weaker Brønsted acidity, and silanols are even weaker sites. Al_{III} sites exhibit stronger Lewis acidity than surface Al_{IV} (obtained upon dehydration of Al-(H_2O) and bonding of the Al_{III} with a close siloxane bridge).[39] Environment effects (confinement induced by van der Waals,

electrostatic and hydrogen bonds) play an important role in the stabilization of the conjugated acid of the basic probe molecule (once protonated or coordinated to aluminum): at the external surface, this leads to adsorption configurations that maximize such interactions.[39,259] CO can be considered as a probe of the local electrostatic field.[38,282] In the case of zeolite beta, it appears that the local electrostatic field (and the CO vibration frequency) remains as high in the open nanopores as in the bulk nanopores and is depleted only at the outermost surface, in particular close to aluminol groups, in a lower extent close to silanols[280] and even less at Al-(H_2O) groups.[38]

To date, calculation of a reaction pathways for proton-catalyzed reactions at the external surface of zeolites are scarce, and so far limited to static approaches, due to the size of the models. Protonation of isobutene was modeled at the surface of zeolite Beta.[38] At the pore mouth, in the open nanopores, bridging OH groups are able to transfer their proton and the carbenium ion is as stable as in the bulk of the zeolite (Figure 8). Alkoxides are also local energy minima, with a better stability as in the bulk, probably because of lower repulsion with the framework, leading to more favorable dispersion interactions. By contrast, Al-(H_2O) species at the outermost surface are not able to stabilize carbenium ions as energy minima. This results from the presence of the aluminol (conjugated base of Al-(H_2O)), which is too basic to afford the stabilization of the highly acidic carbenium and leads to the formation of a C-O bond (thus of an alkoxide). Using embedded cluster models of the ZSM-5 surface exhibiting Si-OH and Al-OH groups, Ferrante et al. investigated the mechanisms of butene isomerization and double-bond migration, that appeared to be more activated for Al-OH than for Si-OH sites.[37] Concerted mechanisms and alkoxide intermediates were invoked. With cluster models exhibiting bridging OH groups, the dehydration of propan-2-ol catalyzed by Brønsted acid sites appears to be less activated in the bulk of ZSM-5 than at the external surface.[254] With periodic models of the external surface of mordenite, Bucko et al.[283] quantified the respective reactivity of mordenite internal and external surface for the

Beckmann rearrangement of cyclohexanone oxime: Si-OH appeared to be less reactive than bridging OH groups from the bulk. The tautomerization of phenol and catechol catalyzed by three-coordinated Al, playing the role of Lewis acid sites, was investigated in the case of ZSM-5 (010) surfaces.[284] Barriers appeared to be quite low, suggesting that this reaction, of interest in the context of lignin transformation, can be catalyzed by ZSM-5 nanosheets. Overall, the presence of open nanopores at the external surface appears to be crucial for the stabilization of charged species generated upon proton transfer, thus for the expression of the acidity.[38-39] In section 6, a comparison will be made with amorphous zones which confirms the need for crystallinity to get strong Brønsted acid sites.

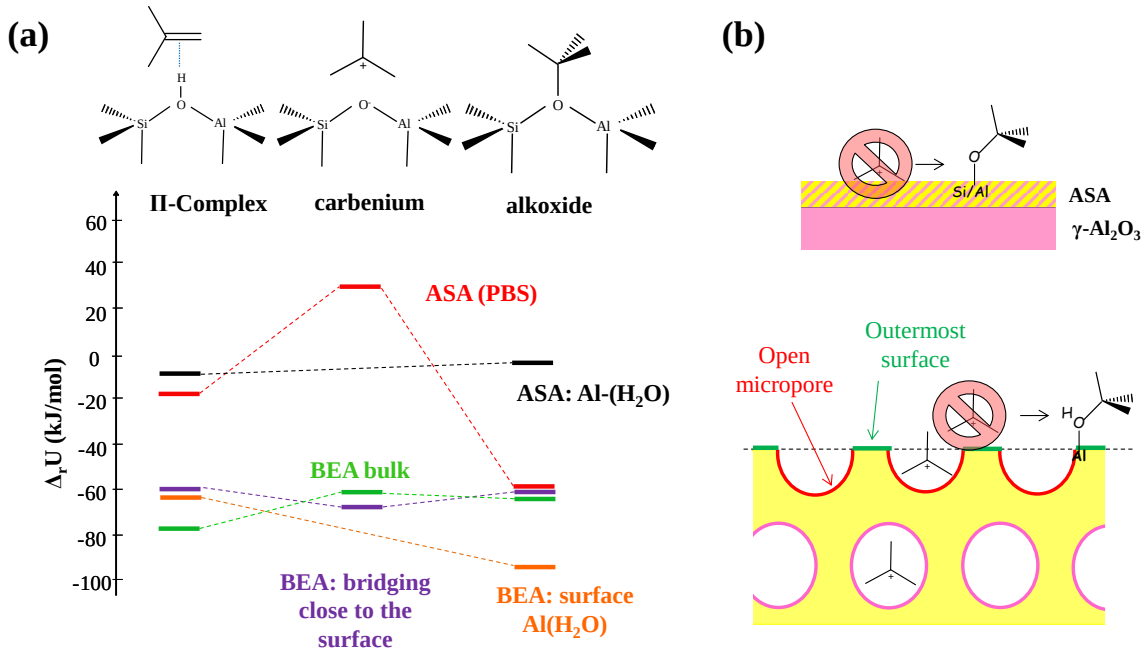

Figure 8. (a) Energy profiles for the protonation of isobutene on ASA (PBS-Al and Al-(H_2O)) and zeolite Beta (selection of bulk and surface sites). Redrawn from data published in ref. [38,285] (b) Scheme depicting the location where the formation of the carbenium ion is possible, versus places where alkoxides only may be formed.

Notably, forcefield investigations (mainly molecular dynamics and grand-canonical Monte Carlo simulations) aiming at simulating adsorption and transport in zeolite slabs reproducing nanosheets or membranes have also been conducted.[267,286-294] Most of the time, purely silicic slabs have been considered. Sometimes, the presence of silanols at the external

surface was also neglected.[287,289-291,293] Insights on the specificity of external surfaces in terms of surface barrier could however be obtained. Concentration profiles and transport properties appeared to be significantly impacted by the presence of the surface.

5.3. Outlooks

So far, most investigations done for the simulations of external surfaces assume one or several surface orientations to be considered, starting from experimental observations. Whereas this is sound to fit to a given observed morphology, this does not help in the definition of the most probable surface orientation that will develop in given synthesis conditions. The most relevant simulation would reproduce the synthesis procedure of zeolites, starting from a model of the precursors solution, in the presence of the template. This has been undertaken by static and AIMD approaches,[20,295-297] but due to the computational cost of this method, the very first steps of the growth could be described, up to the formation of a 4MR,[296] even if larger models have recently been built to understand the interaction between the structure-directing agent and possible Si_{33} precursors in solution.[298] A scale change is clearly required to simulate the growth of particles of realistic sizes. Kinetic Monte Carlo may be an option to propagate the ab initio data obtained for small entities to bigger assemblies.[299] As for the simulation of the formation of defects in zeolites, the question of the regioselectivity of water attack, in terms of internal *versus* external surface, still needs to be addressed. Finally, the investigation of the reactivity of external surface sites is still open, keeping in mind that performing AIMD on external surface models is in principle required, learning from the findings made in reactivity investigations of bulk sites (section 3.3). It remains very challenging due to the size of the cells needed to simulate external surfaces. Addressing at the same time the complexity of the reaction network, and that of the nature of the acid sites, is a current difficulty.

6. AMORPHOUS SILICA-ALUMINA MODELS

Amorphous silica-aluminas (ASAs) are composed of variable amounts of silica, alumina and water. Beside their expected presence as debris in dealuminated zeolites, non-crystaline aluminosilicates are used as acidic catalysts themselves, in particular for the enhancement of the selectivity in middle distillates in hydrocracking reactions,[6,300] and for biomass conversion.[301-305] By contrast to well-crystallized zeolites, the lack of long range ordering in ASA hampers systematic characterization of the local environment around silicon and aluminum. DFT calculations have been performed to shed light on the structure of surface species, on their acidity, and reactivity.

Many works deal with the forcefields or first principles simulation of bulk glassy aluminosilicates,[306-310] but far more scarce are the investigations devoted to the simulation of the surface properties of ASAs. Starting from 2009, I co-published a series of works devoted to the simulation of the interaction of silica derivates with γ-Al_2O_3, and to the deciphering of the acidic properties of ASAs.[40-42,109,282,285,304,311] To the best of my knowledge, this is the first time an ASA surface was modeled, with only a few other attempts afterwards. These achievements are reviewed in the following, and put in perspective with recent experimental findings.

6.1. Construction of the model and OH groups in presence

The grafting of monomeric silicic acid $Si(OH)_4$ was first modeled by exchange with surface OH groups of γ-Al_2O_3.[41] This procedure aimed at reproducing the overall synthesis sequence of ASA samples obtained by deposition of organosilanes $Si(OR)_4$ followed by hydrolysis.[312-314] Starting from the (100) γ-Al_2O_3 surface model built previously by Digne et al.,[315-316] we showed that before thermal treatment (fully hydroxylated surface), no intimate interaction between silica and alumina could be observed. The effect of thermal treatments was deduced from simulations starting from fully dehydrated silicic and alumina systems.

Annealing was simulated by DFT and force-field molecular dynamics. An amorphous surface where silica and alumina are mixed was formed, with a higher proportion of Al_{IV} and Al_V (with respect to Al_{VI}) than on the γ-Al_2O_3 surface, in line with NMR observations.[78,317-318] Then, water adsorption was simulated at various coverage, and the thermodynamic stability of the surface quantified as a function of the temperature and the water partial pressure. Models depicting between 5 and 7 $OH.nm^{-2}$ appeared as relevant (Figures 9-a and b), with a large diversity of OH groups exposed at the surface (Figures 9-c to f). A single bridging OH groups is present (Figure 9-c), bonded to an Al_V (instead of Al_{IV} in the bulk of zeolites) and hydrogen-bond donor to a neighboring oxygen. Silanol groups connected to aluminum atom by Si-O-Al bridges are present (called Silanol-Al, Figure 9-d). Similar structure were proposed by Crépeau et al.[78] Most interestingly, some silanols are tilting toward aluminum atoms, but without any covalent bond:[311] we called these groups aluminic Pseudo-Bridging Silanols (PBS-Al, Figure 9-e). For one of these, a silicon atom plays the role of the acceptor (PBS-Si, Figure 9-f). Also, Al-(H_2O) species could be found on some surface models (Figure 1-e).[40]

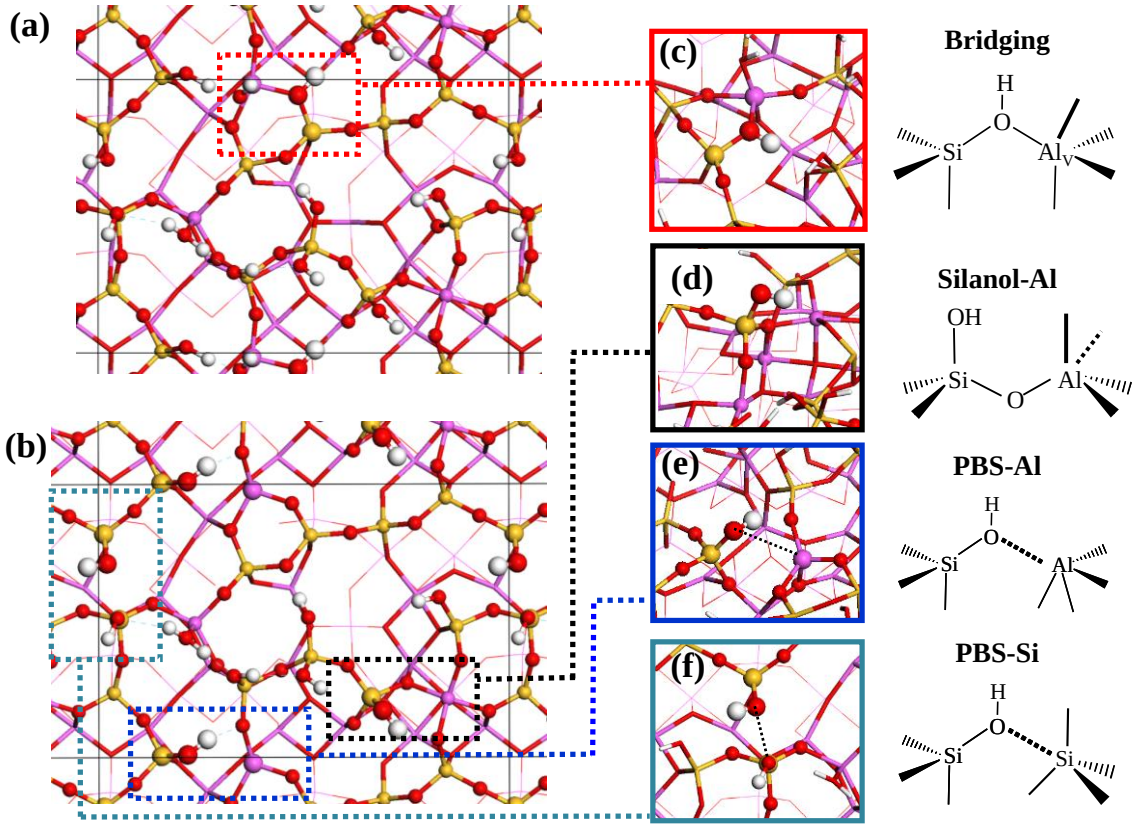

Figure 9. Top view of the ASA surface model first proposed in ref. [41] for (a) θ_{OH} = 6.4 OH nm^{-2}, (b) θ_{OH} = 5.4 OH nm^{-2}; (c) bridging OH group; (d) example of silanol–Al group; (e) example of PBS–Al (PBS: Pseudo-Bridging Silanol); (f) example of PBS–Si. Reproduced with permission from ref. [109]. Copyright 2014, Royal Society of Chemistry.

Other models were proposed in the literature to mimic the grafting of aluminic species on silica models (either crystalline or amorphous).[75,319-321] On some of these models, Al-OH, Al-(H_2O),[319] bridging OH groups[320-321] and pseudo-bridging silanols[320] were observed. Molecular models of hydroxyl groups of ASA were also proposed such as alumino-silsesquioxanes[322-323] and other kinds of clusters:[324-325] even if they cannot considered as representative of a complex amorphous surface, they can be considered as tools to experimentally access the behavior of individual functional groups.

6.2. Spectroscopic validation

A fruitful comparison with spectroscopic (IR, NMR) investigations could be performed. Such spectroscopy studies have a double interest: together with the assignment of

the spectra of ASA samples, a validation of the theoretical model is obtained. The vibration frequencies of OH groups on the ASA surface model were calculated and compared to experiments.[40] The Si-OH frequency, calculated and observed near 3740 cm^{-1} in silica,[326] is lowered when the silanol is in close proximity (Silanol-Al and PBS-Al) with an Al atom. Zeolite-like bridging OH groups on ASA are expected to give rise to a broad and low frequency signal, due to its hydrogen-bond donor nature, explaining why it can only hardly be detected experimentally. The same holds true for most PBS, for which no unambiguous signature can be found due to the strong surface hydrogen-bond network.

Calculated NMR chemical shifts for ^{27}Al and ^{29}Si nuclei present on the model at 5.4 $OH.nm^{-2}$ were compared with advanced dynamic nuclear polarization surface enhanced NMR spectroscopy (DNP SENS) performed on well-controlled silicated alumina samples with variable Si weight.[42] The calculated ^{29}Si chemical shifts of the various surface sites are distributed between –78 to –99 ppm, in good agreement with experiments. On the basis of DFT calculations, we could propose an assignment of the spectra of the Si/Al_2O_3 samples, showing that classical assignments[327-331] in terms of numbers of H and Al as second neighbors, assuming that all oxygen atoms are two-fold coordinated only, are not valid in the present case. This is likely due to the fact that on the model, oxygen atoms can be more than two-fold coordinated due to the higher ionicity of a silicated alumina framework than a silicic one.[311,332-333] Finally, considering DNP SENS scalar refocused INEPT and dipolar refocused R^3-INEPT ^{29}Si–^{27}Al heteronuclear correlation experiments, a critical role of the proximity of silicon nuclei with Al_{IV} in the Brønsted acid sites of ASA is deduced, both through Si-O-Al_{IV} bridges (scalar) and Si-O$\cdots Al_{IV}$ (dipolar) proximities. Together with the PBS structures obtained on the DFT model, this led to the proposal depicted in Figure 1-d. However, we must admit that if calculations are compatible with experiments, certainly some other local structures not reported in our models could be compatible as well. Notably, on the basis of

^{27}Al-{^{1}H} D-HMQC 2D NMR experiments, Huang et al. proposed that non only Al_{IV} atoms can be part of PBS-Al, but also Al_{V}, in line with our calculations.[84]

Hensen et al. showed by H/D exchange of OH groups with deuterated benzene, monitored by FTIR, that bridging OH groups are present on their ASA samples.[72-73] Recently, however, 3D ^{17}O{^{1}H} and 2D ^{17}O{^{1}H,^{27}Al} NMR techniques were developed to estimate O···Al distances in OH groups, found between 3 and 4.4. Å on samples obtained by flame pyrolysis,[83] which compares very well with the O···Al distances measured on our models for a variety of PBS-Al.[41] This strongly reinforces the PBS-Al proposal. No bridging OH groups could be observed in this NMR investigation. Considering the diverging conclusions from experiments regarding the possible existence of bridging and/or pseudo-bridging OH groups from one investigation to another, one may conclude that the nature of OH groups at the surface of ASA strongly depends on the composition (Si/Al ratio) and synthesis mode of the samples.[334] Both proposals (bridging and pseudo-bridging) may be valid.

6.3.Acidity of surface OH groups on ASA

The various surface OH groups obtained on the model were probed by the simulation of the adsorption of CO,[282,311] pyridine,[311] ammonia,[311] and lutidine.[40,311] CO was shown to probe the electrostatic field, proportional to the CO frequency blue-shift as predicted by the vibrational Stark effect. The linear relation appeared to be valid for many alumino-silicates (ASA, zeolites, including external surface sites, silica, alumina).[38,282] PBS-Al sites are at the origin of high electrostatic fields, thus high CO frequency shifts (~35 cm^{-1}), in good agreement with the signal experimentally assigned to strong Brønsted acid sites.[67,72,78] More basic probe molecules able to catch acidic protons, appeared to be able to deprotonate bridging OH groups, PBS-Al, and also PBS-Si groups.[40,311] On PBS sites, this transfer occurs together with the formation of a new Si-O-Al or Si-O-Si bridge, resulting from the reaction of the deprotonated silanolate with the acceptor Al or Si atom. This phenomenon was supposed

to take place by Busca et al. in the case of an Al_{III} acceptor atom.[79] Even if we do not see any Al_{III} on our ASA model, the closing of the "drawbridge"[335] is shown to be relevant with an Al_{IV}, that becomes Al_V after closure of the bridge. Moreover, from NMR experiments, Huang et al. proposed a synergetic effects of several Al_{IV}/Al_V atoms close to the same PBS-Al as a way to get stronger Brønsted acidity.[85,305]

The Al-(H_2O) species present on the ASA model were also shown to be acidic, and to promote the acidity of neighboring silanol groups by cascade proton transfer.[40] This is also in agreement with experimental observations according to which water molecules on ASA contribute to the Brønsted acidity of these.[77,336-337] Generally speaking, the stabilization of the conjugated base of the acid site, and of the protonated probe molecules (i.e., the products of the proton transfer reaction) appeared to be key for the expression of Brønsted acidity of ASA. Whereas these factors also play the role in and on zeolites,[39] the acidity ranking of Al-(H_2O) *versus* bridging OH groups at the external surface of ZSM-5 appeared to be dominated by the intrinsically lower acidity of these two sites. For both sites, the calculations show that the protonated probe molecules will better stabilize in the cavity close to the surface. Thus, the optimal expression of the acidity at the zeolite pore mouth requires to control the degree of crystallinity of the external surface of the zeolite in a very cautious way. Should an amorphous surface be obtained instead, dramatic consequences in terms of depletion of the acidity should be expected.

6.4. Reactivity in acid-catalyzed reactions

The ability of ASA to protonate an alkene (DIB, 2,4,4-trimethyl-2-pentene), and to give rise to cracked products (two isobutene molecules), was then inferred from static estimation of the stability of carbenium *versus* alkoxide species at the ASA surface in comparison with mordenite.[285] The carbocationic pathway is favored in mordenite, whereas on ASA it is strongly activated. On ASA, most sites appeared to be unable (at least, from static calculations) to stabilize a carbenium ion. Only at the PBS-Al sites, a local energy

minimum could be obtained, but with prohibitive energy (illustrated for the case of isobutene in Figure 8-a). Alkoxide ions are much more stable at the ASA surface, and with similar stability with respect to the external surface of zeolite Beta. Thus, for the DIB cracking reaction, PBS-Al sites of ASA promote a tertiary alkoxide route. This was assigned to the electrostatic field, much higher in the zeolite than on ASA.[285]

ASAs are also relevant catalysts for the dehydration of alcohols: we have investigated the ability of the various surface sites to catalyze the production of propene from isopropanol.[304] The PBS-Al site is the only one leading to excellent agreement between measured (103 ± 5 kJ.mol^{-1}) and calculated (104 kJ.mol^{-}1) activation enthalpies. All other sites of the ASA surfaces provide much higher values, thus exhibit much lower reactivity. The analysis of the transition structures (Figure 10) shows that this low activation enthalpy is explained by a synergistic effect between the Lewis and Brønsted acidity simultaneously present at PBS-Al sites. In a concerted step (E2 mechanism), the hydrogen atom of the methyl group is transferred to the neighboring (Si,Al)-μ_2-O; the C-O bond is broken; and the proton from Si-OH is transferred to the OH group of the alcohol. The "OH-" leaving group is thus stabilized at the same time by the Al Lewis acid site and the OH Brønsted acid site. The bridge of the PBS is then closed. Catalysis for alcohol dehydration on ASA is thus primarily Lewis-driven, which is in line with recent spectroscopic findings,[338] but even though the Brønsted moiety does not directly activate the alcohol by protonation, it clearly helps to stabilize the transition state compared to a naked Al_V site from ASA or alumina.[339] From the data calculated ab initio, we constructed a Langmuir-Hinshelwood kinetic model,[304] constructed on the basis of microkinetics schemes deduced for γ-Al_2O_3.[340] The agreement with experiments is good, considering the uncertainty of DFT calculations in terms of adsorption features. Overall, this combined computational and experimental study is certainly the most advanced indication for the relevance of the PBS-Al model.

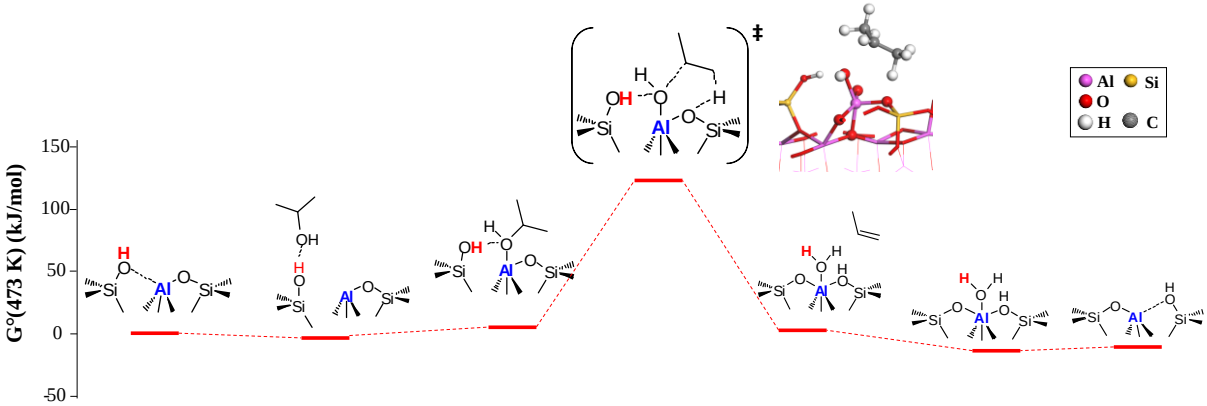

Figure 10. Reaction pathway and Gibbs free energy profile calculated for the formation of propene from isopropanol on PBS-Al sites of the ASA surface model. Inset: representation of the transition state structure. Redrawn from data published in ref. [304].

Comparing the feature of ASA regarding alcohol dehydration with that of crystalline zeolites (see section 3.3.) is then natural. Comparing with the investigation of Reyniers et al. for 1-butanol dehydration into ethers and butenes in various zeolitic frameworks,[209-212] significant mechanistic differences appear with our finding on ASA for isopropanol. We find that ASA is not able to catalyze the formation of ether easily, whereas on zeolites, the importance of a pathway implying ether decomposition for the formation of butene is revealed. The comparison with respect to our results on ASA also suggest that the association of Lewis and Brønsted acidic functions is not invoked or not possible in the surrounding of a perfect bridging OH group of a zeolite. This leads to higher energy barriers (both experimental[341-342] and theoretical[207-212]) within zeolites than on the PBS-Al sites of ASA for the formation of alkenes. The higher reactivity of zeolites with respect to ASA[343] thus needs to be assigned to other factors: concentration of acid sites (a surface density of PBS-Al as low as 0.01-0.1 nm^{-2} - 0.02-0.2 $\mu mol.m^{-2}$ - is expected on silicated alumina investigated in ref. [304]), adsorption features (thanks to confinement effects in zeolites, absent in ASA), or activation entropy parameters (possibly again linked to confinement).

6.5. Outlooks

The possible transferability of specific site structures (in particular PBS-Al) found for silicated alumina, to other kinds of amorphous aluminosilicate structures, needs to be investigated. In particular, the case of silica-rich entities is of interest, when dealing with amorphous entities present after zeolite synthesis or post-treatments. So far, on the models built for the external surfaces of zeolites, no PBS site could be observed (section 5). Thus, a certain level of disorder seems to be required to obtain such species: the situation of a poorly crystalline zeolite surface could be somewhere in-between ordered surfaces and fully amorphous zones. As for other kinds of defects, the evaluation of the reactivity of ASA at a higher level of theory and with molecular dynamics is required, but currently very challenging, again due to the size of the cells.

7. SUMMARY AND GENERAL OUTLOOKS

This Perspective illustrates how computational chemistry helps in bringing atomic-scale information on the sources of complexity that make a real acidic zeolite catalyst an intricate system. Unequaled level of knowledge were obtained on the structure of defects such as EFAl, on the mechanism of their formation upon water attack, about the surface sites present at the external surfaces of zeolites and on amorphous silica-alumina. Consequences on acidity and reactivity were also reviewed. The gap is however still large between the current achievements in the field of simulation of intricate zeolite catalysts, and the full description of an industrial-like catalyst.

As mentioned in section 1, shaping of the zeolites is required before industrial use. Aluminum and other ions migration, genesis of new acid sites, pore blockage, are likely occurring due to the zeolite / binder interaction, with impact on the catalyst activity, selectivity and deactivation properties.[95,97,99-102] To address such a question, the structure of the external surface of zeolite crystallites (the main contact zone with the binder) has to be known first, before its interaction with the binder can be investigated. From the computational

point of view, this last aspect was never addressed so far to the best of my knowledge, which justifies a research program in that direction in the future.

Many industrial zeolite catalysts are actually bifunctional. The acidic function of zeolites is beneficially combined to another active phase (e.g. a metal, or a metallic sulfide), which expands the capacity of zeolites to transform poorly reactive molecules (such as alkanes) thanks to pre-activation by the co-catalyst (upon dehydrogenation into alkenes for example).[344-345] The later may be deposited either on the binder, either on the zeolite itself.[346-348] In some cases, but not all, the location of the metallic phase with respect to the acidic phase plays a role in the catalytic performance, that needs to be elucidated. Confinement effects, pore mouth catalysis and diffusion limitations may all play a role in that respect.[167,347-349] From a computational point of view, several teams established some models for small metallic particles (from 1 to 6 atoms) occluded within the nanopores of zeolites,[206,350-353] in particular in the case of platinum.[354-358] Advanced models of platinum-based metallic particles supported on γ-Al_2O_3 (frequently used as a binder) have also been proposed,[359-364] and they dehydrogenation ability investigated.[365-366] All these investigations pave the way for a better understanding of the bifunctional mechanisms into play, and on the impact on the support (either the binder, either the zeolite) on the reactivity of the metallic phase.

Then, quantifying the effect of diffusion limitations by computational chemistry requires to undertake higher scale simulations. Forcefield approaches have been reported to deduce diffusion coefficients of various molecules in zeolites, in particular by molecular dynamics.[24] The impact of external surfaces was quantified in a few cases (see section 5.2), but generally speaking the effect of defects was not quantified. These properties are moreover not converted into components of the apparent reaction rate, as mechanistic and diffusion investigations are performed with different tools. Diffusion induces limitations in apparent reaction rate. Thus, there is a urgent need to integrate diffusion and reaction limitations in unified kinetic models.

Many other sources of complexity of acidic zeolite-based industrial catalysts, from the atomic to the particle size, could be listed, such as the presence of other elements than Si or Al (in framework or extra-framework positions), or the interconnected nano/meso/macropore systems, that all play a role in the performance. Reaching a full understanding and prediction ability of these systems will require multi-scale approaches, both experimentally and computationally speaking.

AUTHOR INFORMATION

Corresponding Author:

* Céline Chizallet, IFP Energies nouvelles, celine.chizallet@ifpen.fr

ACKNOWLEDGEMENTS.

I warmly thank all the colleagues, students and collaborators that have worked with me on the topic covered by this Perspective, in particular Pascal Raybaud, Fabien Leydier, Marius-Christian Silaghi, Elena Petracovschi, Jérôme Rey, Laureline Treps, Kim Larmier, Ester Gutierrez-Acebo, Theodorus de Bruin, Christophe Bouchy, Axel Gomez, Nicolas Cadran, Sylvie Maury (at IFP Energies nouvelles), Joachim Sauer (Humboldt Universität Berlin), Tomas Bucko (Comenius University Bratislava), Dominique Costa (Chimie Paris Tech), Hélène Lauron-Pernot, Eric Marceau (Sorbonne Université), Christophe Copéret, Jeroen van Bokhoven (ETH-Zürich), Y. Schuurman (IRCELYON). I also thank IFP Energies nouvelles and Collaborative Research Center 1109 ‘‘Understanding of Metal Oxide/Water Systems at the Molecular Scale: Structural Evolution, Interfaces, and Dissolution”, funded by the DFG, for support. This work has been partly supported by the Common Research laboratory CARMEN (ENS de Lyon, CNRS, IFPEN, Claude Bernard Lyon 1 University, Sorbonne University and University of Strasbourg).

Table of Contents artwork

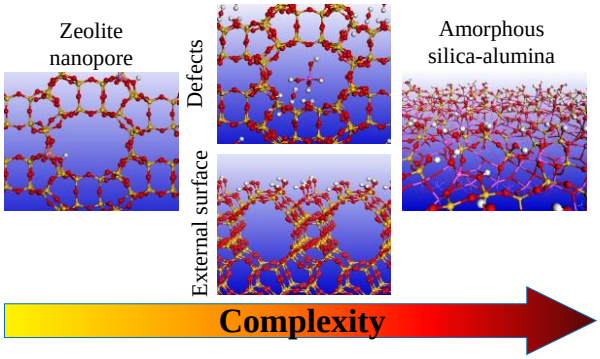

REFERENCES.

(1) Li, Y.; Yu, J., New Stories of Zeolite Structures: Their Descriptions, Determinations, Predictions, and Evaluations, *Chem. Rev.* **2014**, *114*, 7268-7316.
(2) Li, J.; Corma, A.; Yu, J., Synthesis of New Zeolite Structures, *Chem. Soc. Rev.* **2015**, *44*, 7112-7127.
(3) Baerlocher, C.; McCusker, J. K., *Database of Zeolite Structures:* http://www.iza-structure.org/databases/.
(4) Davis, M. E., Ordered Porous Materials for Emerging Applications, *Nature* **2002**, *417*, 813-821.
(5) Corma, A., Inorganic Solid Acids and their Use in Acid-Catalyzed Hydrocarbon Reactions, *Chem. Rev.* **1995**, *95*, 559-614.
(6) Marcilly, C. *Acido-Basic Catalysis*; Technip: Paris, 2005.
(7) Vermeiren, W.; Gilson, J. P., Impact of Zeolites on the Petroleum and Petrochemical Industry, *Topics Catal.* **2009**, *52*, 1131-1161.
(8) Vogt, E. T. C.; Weckhuysen, B. M., Fluid Catalytic Cracking: Recent Developments on the Grand Old Lady of Zeolite Catalysis, *Chem. Soc. Rev.* **2015**, *44*, 7342-7370.
(9) Deka, U.; Lezcano-Gonzalez, I.; Weckhuysen, B. M.; Beale, A. M., Local Environment and Nature of Cu Active Sites in Zeolite-Based Catalysts for the Selective Catalytic Reduction of NOx, *ACS Catal.* **2013**, *3*, 413-427.
(10) Borfecchia, E.; Beato, P.; Svelle, S.; Olsbye, U.; Lamberti, C.; Bordiga, S., Cu-CHA – A Model System for Applied Selective Redox Catalysis, *Chem. Soc. Rev.* **2018**, *47*, 8097-8133.
(11) Paolucci, C.; Khurana, I.; Parekh, A. A.; Li, S.; Shih, A. J.; Li, H.; Di Iorio, J. R.; Albarracin-Caballero, J. D.; Yezerets, A.; Miller, J. T.; Delgass, W. N.; Ribeiro, F. H.; Schneider, W. F.; Gounder, R., Dynamic Multinuclear Sites Formed by Mobilized Copper Ions in NOx Selective Catalytic Reduction, *Science* **2017**, *357*, 898-903.
(12) Ennaert, T.; Van Aelst, J.; Dijkmans, J.; De Clercq, R.; Schutyser, W.; Dusselier, M.; Verboekend, D.; Sels, B. F., Potential and Challenges of Zeolite Chemistry in the Catalytic Conversion of Biomass, *Chem. Soc. Rev.* **2016**, *45*, 584-611.
(13) Jae, J.; Tompsett, G. A.; Foster, A. J.; Hammond, K. D.; Auerbach, S. M.; Lobo, R. F.; Huber, G. W., Investigation into the Shape Selectivity of Zeolite Catalysts for Biomass Conversion, *J. Catal.* **2011**, *279*, 257-268.
(14) Delidovich, I.; Palkovits, R., Catalytic Isomerization of Biomass-Derived Aldoses: A Review, *ChemSusChem* **2016**, *9*, 547-561.
(15) Serrano, D. P.; Melero, J. A.; Morales, G.; Iglesias, J.; Pizarro, P., Progress in the Design of Zeolite Catalysts for Biomass Conversion into Biofuels and Bio-Based Chemicals, *Catal. Rev.* **2018**, *60*, 1-70.
(16) Sauer, J., Molecular Models in ab Initio Studies of Solids and Surfaces: From Ionic Crystals and Semiconductors to Catalysts, *Chem. Rev.* **1989**, *89*, 199-255.
(17) van Santen, R.; Kramer, G. J., Reactivity Theory of Zeolitic Brønsted Acidic Sites, *Chem. Rev.* **1995**, *95*, 637-660.
(18) Farneth, W. E.; Gorte, R. J., Methods for Characterizing Zeolite Acidity, *Chem. Rev.* **1995**, *95*, 615-635.
(19) Busca, G., Acid Catalysts in Industrial Hydrocarbon Chemistry, *Chem. Rev.* **2007**, *107*, 5366-5410.
(20) Van Speybroeck, V.; Hemelsoet, K.; Joos, L.; Waroquier, M.; Bell, R. G.; Catlow, C. R. A., Advances in Theory and their Application within the Field of Zeolite Chemistry, *Chem. Soc. Rev.* **2015**, *44*, 7044-7111.
(21) Boronat, M.; Corma, A., Factors Controlling the Acidity of Zeolites, *Catal. Lett.* **2015**, *145*, 162-172.
(22) Grajciar, L.; Heard, C. J.; Bondarenko, A. A.; Polynski, M. V.; Meeprasert, J.; Pidko, E. A.; Nachtigall, P., Towards Operando Computational Modeling in Heterogeneous Catalysis, *Chem. Soc. Rev.* **2018**, *47*, 8307-8348.
(23) Derouane, E. G.; André, J. M.; Lucas, A. A., Surface Curvature Effects in Physisorption and Catalysis by Microporous Solids and Molecular Sieves, *J. Catal.* **1988**, *110*, 58-73.

(24) Smit, B.; Maesen, T., Molecular Simulations of Zeolites: Adsorption, Diffusion, and Shape Selectivity, *Chem. Rev.* **2008**, *108*, 4125–4184.
(25) Weisz, P. B.; Frilette, V. J., Intracrystalline and Molecular-Shape-Selective Catalysis by Zeolite Salts, *J. Phys. Chem.* **1960**, *64*, 382-382.
(26) Weisz, P. B.; Frilette, V. J.; Maatman, R. W.; Mower, E. B., Catalysis by Crystalline Aluminosilicates II. Molecular-Shape Selective Reactions, *J. Catal.* **1962**, *1*, 307-312.
(27) Smit, B.; Maesen, T. L. M., Towards a Molecular Understanding of Shape Selectivity, *Nature* **2008**, *451*, 671-678.
(28) Lin, L.-C.; Berger, A. H.; Martin, R. L.; Kim, J.; Swisher, J. A.; Jariwala, K.; Rycroft, C. H.; Bhown, A. S.; Deem, M. W.; Haranczyk, M.; Smit, B., In Silico Screening of Carbon-Capture Materials, *Nat. Mater.* **2012**, *11*, 633-641.
(29) Yarulina, I.; De Wispelaere, K.; Bailleul, S.; Goetze, J.; Radersma, M.; Abou-Hamad, E.; Vollmer, I.; Goesten, M.; Mezari, B.; Hensen, E. J. M.; Martínez-Espín, J. S.; Morten, M.; Mitchell, S.; Perez-Ramirez, J.; Olsbye, U.; Weckhuysen, B. M.; Van Speybroeck, V.; Kapteijn, F.; Gascon, J., Structure–Performance Descriptors and the Role of Lewis Acidity in the Methanol-to-Propylene Process, *Nature Chem.* **2018**, *10*, 804-812.
(30) Gallego, E. M.; Portilla, M. T.; Paris, C.; León-Escamilla, A.; Boronat, M.; Moliner, M.; Corma, A., "Ab initio" Synthesis of Zeolites for Preestablished Catalytic Reactions, *Science* **2017**, *355*, 1051–1054.
(31) Bai, P.; Jeon, M. Y.; Ren, L.; Knight, C.; Deem, M. W.; Tsapatsis, M.; Siepmann, J. I., Discovery of Optimal Zeolites for Challenging Separations and Chemical Transformations using Predictive Materials Modeling, *Nat. Commun.* **2015**, *6*, 5912.
(32) Uytterhoeven, J. B.; Christner, L. G.; Hall, W. K., Studies of the Hydrogen Held by Solids. VIII. The Decationated Zeolites, *J. Phys. Chem.* **1965**, *69*, 2117-2126.
(33) Haag, W. O.; Lago, R. M.; Weisz, P. B., The Active Site of Acidic Aluminosilicate Catalysts, *Nature* **1984**, *309*, 589-591.
(34) Mortier, W. J.; Sauer, J.; Lercher, J. A.; Noller, H., Bridging and Terminal Hydroxyls. A Structural Chemical and Quantum Chemical Discussion, *J. Phys. Chem.* **1984**, *88*, 905-912.
(35) Bucko, T.; Benco, L.; Demuth, T.; Hafner, J., Ab Initio Density Functional Investigation of the (001) Surface of Mordenite, *J. Chem. Phys.* **2002**, *117*, 7295-7305.
(36) Hernandez-Tamargo, C. E.; Roldan, A.; de Leeuw, N. H., A Density Functional Theory Study of the Structure of Pure-Silica and Aluminium-Substituted MFI Nanosheets, *J. Solid State Chem.* **2016**, *237*, 192-203.
(37) Ferrante, F.; Rubino, T.; Duca, D., Butene Isomerization and Double-Bond Migration on the H-ZSM-5 Outer Surface: A Density Functional Theory Study, *J. Phys. Chem. C* **2011**, *115*, 14862-14868.
(38) Rey, J.; Raybaud, P.; Chizallet, C., Ab Initio Simulation of the Acid Sites at the External Surface of Zeolite Beta, *ChemCatChem* **2017**, *9*, 2176-2185.
(39) Treps, L.; Gomez, A.; De Bruin, T.; Chizallet, C., Environment, Stability and Acidity of External Surface Sites of Silicalite-1 and ZSM-5 Micro- and Nano-Slabs, -Sheets and -Crystals, *ACS Catal.* **2020**, *10*, 3297−3312.
(40) Leydier, F.; Chizallet, C.; Chaumonnot, A.; Digne, M.; Soyer, E.; Quoineaud, A. A.; Costa, D.; Raybaud, P., Brønsted Acidity of Amorphous Silica–Alumina: The Molecular Rules of Proton Transfer, *J. Catal.* **2011**, *284*, 215-229.
(41) Chizallet, C.; Raybaud, P., Pseudo-Bridging Silanols as Versatile Brønsted Acid Sites of Amorphous Aluminosilicates Surfaces, *Angew. Chem. Int. Ed.* **2009**, *48*, 2891-2893.
(42) Valla, M.; Rossini, A. J.; Caillot, M.; Chizallet, C.; Raybaud, P.; Digne, M.; Chaumonnot, A.; Lesage, A.; Emsley, L.; van Bokhoven, J. A.; Coperet, C., Atomic Description of the Interface between Silica and Alumina in Aluminosilicates through Dynamic Nuclear Polarization Surface-Enhanced NMR Spectroscopy and First-Principles Calculations, *J. Am. Chem. Soc.* **2015**, *137*, 10710-10719.
(43) Roeffaers, M. B. J.; Ameloot, R.; Baruah, M.; Uji-i, H.; Bulut, M.; De Cremer, G.; Müller, U.; Jacobs, P. A.; Hofkens, J.; Sels, B. F.; De Vos, D. E., Morphology of Large ZSM-5 Crystals Unraveled by Fluorescence Microscopy, *J. Am. Chem. Soc.* **2008**, *130*, 5763–5772.
(44) Karwacki, L.; Kox, M. H. F.; Matthijs de Winter, D. A.; Drury, M. R.; Meeldijk, J. D.; Stavitski, E.; Schmidt, W.; Mertens, M.; Cubillas, P.; John, N.; Chan, A.; Kahn, N.; Bare, S. R.;

Anderson, M.; Kornatowski, J.; Weckhuysen, B. M., Morphology-Dependent Zeolite Intergrowth Structures Leading to Distinct Internal and Outer-Surface Molecular Diffusion Barriers, *Nat. Mater.* **2009**, *8*, 959.
(45) Mintova, S.; Jaber, M.; Valtchev, V., Nanosized Microporous Crystals: Emerging Applications, *Chem. Soc. Rev.* **2015**, *44*, 7207-7233.
(46) Grand, J.; Talapaneni, S. N.; Vicente, A.; Fernandez, C.; Dib, E.; Aleksandrov, H. A.; Vayssilov, G. N.; Retoux, R.; Boullay, P.; Gilson, J.-P.; Valtchev, V.; Mintova, S., One-Pot Synthesis of Silanol-Free Nanosized MFI Zeolite, *Nat. Mater.* **2017**, *16*, 1010-1015.
(47) Jacobs, P. A.; Derouane, E. G.; Weitkamp, J., Evidence for X-Ray-Amorphous Zeolites, *J. Chem. Soc., Chem. Commun.* **1981**, 591-593.
(48) Haw, K.-G.; Gilson, J.-P.; Nesterenko, N.; Akouche, M.; El Siblani, H.; Goupil, J.-M.; Rigaud, B.; Minoux, D.; Dath, J.-P.; Valtchev, V., Supported Embryonic Zeolites and their Use to Process Bulky Molecules, *ACS Catal.* **2018**, *8*, 8199-8212.
(49) Choi, M.; Na, K.; Kim, J.; Sakamoto, Y.; Terasaki, O.; Ryoo, R., Stable Single-Unit-Cell Nanosheets of Zeolite MFI as Active and Long-Lived Catalysts, *Nature* **2009**, *461*, 246-249.
(50) Kirschhock, C. E. A.; Kremer, S. P. B.; Vermant, J.; Van Tendeloo, G.; Jacobs, P. A.; Martens, J. A., Design and Synthesis of Hierarchical Materials from Ordered Zeolitic Building Units, *Chem. Eur. J.* **2005**, *11*, 4306-4313.
(51) Roth, W. J.; Nachtigall, P.; Morris, R. E.; Čejka, J., Two-Dimensional Zeolites: Current Status and Perspectives, *Chem. Rev.* **2014**, *114*, 4807-4837.
(52) Buchner, C.; Lichtenstein, L.; Yu, X.; Boscoboinik, J. A.; Yang, B.; Kaden, W. E.; Heyde, M.; Shaikhutdinov, S. K.; Wlodarczyk, R.; Sierka, M.; Sauer, J.; Freund, H. J., Ultrathin Silica Films: the Atomic Structure of Two-Dimensional Crystals and Glasses, *Chemistry* **2014**, *20*, 9176-9183.
(53) Bordiga, S.; Lamberti, C.; Bonino, F.; Travert, A.; Thibault-Starzyk, F., Probing Zeolites by Vibrational Spectroscopies, *Chem. Soc. Rev.* **2015**, *44*, 7262-7341.
(54) Martens, J. A.; Vanbutsele, G.; Jacobs, P. A.; Denayer, J.; Ocakoglu, R.; Baron, G.; Muñoz Arroyo, J. A.; Thybaut, J.; Marin, G. B., Evidences for Pore Mouth and Key–Lock Catalysis in Hydroisomerization of Long n-Alkanes over 10-Ring Tubular Pore Bifunctional Zeolites, *Catal. Today* **2001**, *65*, 111-116.
(55) Martens, J. A.; Souverijns, W.; Verrelst, W.; Parton, R.; Froment, G. F.; Jacobs, P. A., Selective Isomerization of Hydrocarbon Chains on External Surfaces of Zeolite Crystals, *Angew. Chem. Int. Ed.* **1995**, *34*, 2528-2530.
(56) Valtchev, V.; Majano, G.; Mintova, S.; Perez-Ramirez, J., Tailored Crystalline Microporous Materials by Post-Synthesis Modification, *Chem. Soc. Rev.* **2013**, *42*, 263-290.
(57) Perez-Ramirez, J.; Christensen, C. H.; Egeblad, K.; Christensen, C. H.; Groen, J. C., Hierarchical Zeolites: Enhanced Utilisation of Microporous Crystals in Catalysis by Advances in Materials Design, *Chem. Soc. Rev.* **2008**, *37*, 2530-2542.
(58) Silaghi, M.-C.; Chizallet, C.; Raybaud, P., Challenges on Molecular Aspects of Dealumination and Desilication of Zeolites, *Microporous Mesoporous Mater.* **2014**, *191*, 82-96.
(59) Přech, J.; Pizarro, P.; Serrano, D. P.; Čejka, J., From 3D to 2D Zeolite Catalytic Materials, *Chem. Soc. Rev.* **2018**, *47*, 8263-8306.
(60) Mitchell, S.; Pinar, A. B.; Kenvin, J.; Crivelli, P.; Karger, J.; Perez-Ramirez, J., Structural Analysis of Hierarchically Organized Zeolites, *Nat. Commun.* **2015**, *6*, 8633.
(61) van Donk, S.; Janssen, A. H.; Bitter, J. H.; de Jong, K. P., Generation, Characterization, and Impact of Mesopores in Zeolite Catalysts, *Catal. Rev.* **2003**, *45*, 297-319.
(62) Karwacki, L.; de Winter, D. A. M.; Aramburo, L. R.; Lebbink, M. N.; Post, J. A.; Drury, M. R.; Weckhuysen, B. M., Architecture-Dependent Distribution of Mesopores in Steamed Zeolite Crystals as Visualized by FIB-SEM Tomography, *Angew. Chem. Int. Ed.* **2011**, *50*, 1294-1298.
(63) van Bokhoven, J. A.; van der Eerden, A. M. J.; Koningsberger, D. C., Three-Coordinate Aluminum in Zeolites Observed with In situ X-ray Absorption Near-Edge Spectroscopy at the Al K-Edge: Flexibility of Aluminum Coordinations in Zeolites, *J. Am. Chem. Soc.* **2003**, *125*, 7435-7442.
(64) Agostini, G.; Lamberti, C.; Palin, L.; Milanesio, M.; Danilina, N.; Xu, B.; Janousch, M.; van Bokhoven, J. A., In Situ XAS and XRPD Parametric Rietveld Refinement To Understand Dealumination of Y Zeolite Catalyst, *J. Am. Chem. Soc.* **2010**, *132*, 667-678.

(65) Pellet, R. J.; Blackwell, C. S.; Rabo, J. A., Catalytic Cracking Studies and Characterization of Steamed Y and LZ-210 Zeolites, *J. Catal.* **1988**, *114*, 71-89.
(66) Barthomeuf, D., ASA Debris in Zeolites and Zeolitic-Type Clusters in ASA Catalysts, *Zeolites* **1990**, *10*, 131-133.
(67) Cairon, O.; Chevreau, T.; Lavalley, J. C., Brønsted Acidity of Extraframework Debris in Steamed Y Zeolites from the FTIR Study of CO Adsorption, *J. Chem. Soc., Faraday Trans.* **1998**, *94*, 3039-3047.
(68) Menezes, S. M. C.; Camorim, V. L.; Lam, Y. L.; San Gil, R. A. S.; Bailly, A.; Amoureux, J. P., Characterization of Extra-Framework Species of Steamed and Acid Washed Faujasite by MQMAS NMR and IR Measurements, *Appl. Catal. A* **2001**, *207*, 367-377.
(69) Omegna, A.; Prins, R.; van Bokhoven, J. A., Effect of Temperature on Aluminum Coordination in Zeolites H-Y and H-USY and Amorphous Silica Alumina: an *in situ* Al K Edge XANES Study, *J. Phys. Chem. B* **2005**, *109*, 9280-9283.
(70) Matsunaga, Y.; Yamazaki, H.; Yokoi, T.; Tatsumi, T.; Kondo, J. N., IR Characterization of Homogeneously Mixed Silica–Alumina Samples and Dealuminated Y Zeolites by Using Pyridine, CO, and Propene Probe Molecules, *J. Phys. Chem. C* **2013**, *117*, 14043-14050.
(71) Benazzi, E.; Leite, L.; Marchal-George, N.; Toulhoat, H.; Raybaud, P., New Insights into Parameters Controlling the Selectivity in Hydrocracking Reactions, *J. Catal.* **2003**, *217*, 376-387.
(72) Hensen, E. J. M.; Poduval, D. G.; Degirmenci, V.; Ligthart, D. A. J. M.; Chen, W.; Maugé, F.; Rigutto, M. S.; van Veen, J. A. R., Acidity Characterization of Amorphous Silica–Alumina, *J. Phys. Chem. C* **2012**, *116*, 21416-21429.
(73) Poduval, D. G.; van Veen, J. A. R.; Rigutto, M. S.; Hensen, E. J. M., Brønsted Acid Sites of Zeolitic Strength in Amorphous Silica-Alumina, *Chem. Commun.* **2010**, *46*, 3466-3468.
(74) Gora-Marek, K.; Derewinski, M.; Sarv, P.; Datka, J., IR and NMR Studies of Mesoporous Alumina and Related Aluminosilicates, *Catal. Today* **2005**, *101*, 131-138.
(75) Yun, D.; Yun, Y. S.; Kim, T. Y.; Park, H.; Lee, J. M.; Han, J. W.; Yi, J., Mechanistic Study of Glycerol Dehydration on Brønsted Acidic Amorphous Aluminosilicate, *J. Catal.* **2016**, *341*, 33-43.
(76) Hunger, M.; Freunde, D.; Pfeifer, H.; Bremer, H.; Jank, M.; Wendlandt, K. P., High-Resolution Proton Magnetic Resonance and Catalytic Studies Concerning Brønsted Centers of Amorphous Al_2O_3-SiO_2 Solids, *Chem. Phys. Lett.* **1983**, *100*, 29-33.
(77) Williams, M. F.; Fonfé, B.; Sievers, C.; Abraham, A.; van Bokhoven, J. A.; Jentys, A.; van Veen, J. A. R.; Lercher, J. A., Hydrogenation of Tetralin on Silica–Alumina-Supported Pt Catalysts. I. Physicochemical Characterization of the Catalytic Materials, *J. Catal.* **2007**, *251*, 485-496.
(78) Crépeau, G.; Montouillout, V.; Vimont, A.; Mariey, L.; Cseri, T.; Maugé, F., Nature, Structure and Strength of the Acidic Sites of Amorphous Silica Alumina: an IR and NMR Study, *J. Phys. Chem. B* **2006**, *110*, 15172-15185.
(79) Trombetta, M.; Busca, G.; Rossini, S.; Piccoli, V.; Cornaro, U.; Guercio, A.; Catani, R.; Willey, R. J., FT-IR Studies on Light Olefin Skeletal Isomerization , III. Surface Acidity and Activity of Amorphous and Crystalline Catalysts Belonging to the SiO_2–Al_2O_3 System, *J. Catal.* **1998**, *179*, 581-596.
(80) Daniell, W.; Schubert, U.; Glöckler, R.; Meyer, A.; Noweck, K.; Knözinger, H., Enhanced Surface Acidity in Mixed Alumina–Silicas: a Low-Temperature FTIR Study, *Appl. Catal. A* **2000**, *196*, 247-260.
(81) Phung, T. K.; Busca, G., Ethanol Dehydration on Silica-Aluminas: Active Sites and Ethylene/Diethyl Ether Selectivities, *Catal. Comm.* **2015**, *68*, 110-115.
(82) Baca, M.; De la Rochefoucauld, E.; Ambroise, E.; Krafft, J. M.; Hajjar, R.; Man, P. P.; Carrier, X.; Blanchard, J., Characterization of Mesoporous Alumina Prepared by Surface Alumination of SBA-15, *Microporous Mesoporous Mater.* **2008**, *110*, 232-241.
(83) Perras, F. A.; Wang, Z.; Kobayashi, T.; Baiker, A.; Huang, J.; Pruski, M., Shedding Light on the Atomic-Scale Structure of Amorphous Silica–Alumina and its Brønsted Acid Sites, *Phys. Chem. Chem. Phys.* **2019**, *21*, 19529-19537.
(84) Wang, Z.; Jiang, Y.; Lafon, O.; Trébosc, J.; Duk Kim, K.; Stampfl, C.; Baiker, A.; Amoureux, J.-P.; Huang, J., Brønsted Acid Sites Based on Penta-Coordinated Aluminum Species, *Nat. Commun.* **2016**, *7*, 13820.

(85) Huang, J.; van Vegten, N.; Jiang, Y.; Hunger, M.; Baiker, A., Increasing the Bronsted Acidity of Flame-Derived Silica/Alumina up to Zeolitic Strength, *Angew. Chem., Int. Ed* **2010**, *49*, 7776-7781.
(86) Sanchez Escribano, V.; Garbarino, G.; Finocchio, E.; Busca, G., γ-Alumina and Amorphous Silica–Alumina: Structural Features, Acid Sites and the Role of Adsorbed Water, *Topics Catal.* **2017**, *60*, 1554-1564.
(87) Rankin, A. G. M.; Webb, P. B.; Dawson, D. M.; Viger-Gravel, J.; Walder, B. J.; Emsley, L.; Ashbrook, S. E., Determining the Surface Structure of Silicated Alumina Catalysts via Isotopic Enrichment and Dynamic Nuclear Polarization Surface-Enhanced NMR Spectroscopy, *J. Phys. Chem. C* **2017**, *121*, 22977-22984.
(88) Goldsmith, B. R.; Peters, B.; Johnson, J. K.; Gates, B. C.; Scott, S. L., Beyond Ordered Materials: Understanding Catalytic Sites on Amorphous Solids, *ACS Catal.* **2017**, *7*, 7543-7557.
(89) Ardagh, M. A.; Bo, Z.; Nauert, S. L.; Notestein, J. M., Depositing SiO_2 on Al_2O_3: a Route to Tunable Brønsted Acid Catalysts, *ACS Catal.* **2016**, *6*, 6156-6164.
(90) Parker, W. O. N.; Wegner, S., Aluminum in Mesoporous Silica–Alumina, *Microporous Mesoporous Mater.* **2012**, *158*, 235-240.
(91) Haw, K.-G.; Goupil, J.-M.; Gilson, J.-P.; Nesterenko, N.; Minoux, D.; Dath, J.-P.; Valtchev, V., Embryonic ZSM-5 Zeolites: Zeolitic Materials with Superior Catalytic Activity in 1,3,5-Triisopropylbenzene Dealkylation, *New J. Chem.* **2016**, *40*, 4307-4313.
(92) Hargreaves, J. S. J.; Munnoch, A. L., A Survey of the Influence of Binders in Zeolite Catalysis, *Catal. Sci. Technol.* **2013**, *3*, 1165-1171.
(93) Mitchell, S.; Michels, N.-L.; Perez-Ramirez, J., From Powder to Technical Body: the Undervalued Science of Catalyst Scale Up, *Chem. Soc. Rev.* **2013**, *42*, 6094-6112.
(94) Bingre, R.; Louis, B.; Nguyen, P., An Overview on Zeolite Shaping Technology and Solutions to Overcome Diffusion Limitations, *Catalysts* **2018**, *8*, 163.
(95) Whiting, G. T.; Meirer, F.; Mertens, M. M.; Bons, A.-J.; Weiss, B. M.; Stevens, P. A.; de Smit, E.; Weckhuysen, B. M., Binder Effects in SiO_2- and Al_2O_3-Bound Zeolite ZSM-5-Based Extrudates as Studied by Microspectroscopy, *ChemCatChem* **2015**, *7*, 1312-1321.
(96) Mitchell, S.; Michels, N.-L.; Kunze, K.; Pérez-Ramírez, J., Visualization of Hierarchically Structured Zeolite Bodies from Macro to Nano Length Scales, *Nature Chem.* **2012**, *4*, 825-831.
(97) Michels, N.-L.; Mitchell, S.; Pérez-Ramírez, J., Effects of Binders on the Performance of Shaped Hierarchical MFI Zeolites in Methanol-to-Hydrocarbons, *ACS Catal.* **2014**, *4*, 2409-2417.
(98) da Silva, J. C.; Mader, K.; Holler, M.; Haberthur, D.; Diaz, A.; Guizar-Sicairos, M.; Cheng, W. C.; Shu, Y.; Raabe, J.; Menzel, A.; van Bokhoven, J. A., Assessment of the 3 D Pore Structure and Individual Components of Preshaped Catalyst Bodies by X-Ray Imaging, *ChemCatChem* **2015**, *7*, 413-416.
(99) Whiting, G. T.; Chung, S.-H.; Stosic, D.; Chowdhury, A. D.; van der Wal, L. I.; Fu, D.; Zecevic, J.; Travert, A.; Houben, K.; Baldus, M.; Weckhuysen, B. M., Multiscale Mechanistic Insights of Shaped Catalyst Body Formulations and Their Impact on Catalytic Properties, *ACS Catal.* **2019**, *9*, 4792-4803.
(100) Chang, C. D.; Hellring, S. D.; Miale, J. N.; Schmitt, K. D.; Brigandi, P. W.; Wu, E. L., Insertion of Aluminium into High-Silica-Content Zeolite Frameworks. Part 3.-Hydrothermal Transfer of Aluminium from Al_2O_3 into [Al]ZSM-5 and [B]ZSM-5, *J. Chem. Soc., Faraday Trans. 1* **1985**, *81*, 2215-2224.
(101) Shihabi, D. S.; Garwood, W. E.; Chu, P.; Miale, J. N.; Lago, R. M.; Chu, C. T. W.; Chang, C. D., Aluminum Insertion into High-Silica Zeolite Frameworks: II. Binder Activation of High-Silica ZSM-5, *J. Catal.* **1985**, *93*, 471-474.
(102) Lakiss, L.; Gilson, J.-P.; Valtchev, V.; Mintova, S.; Vicente, A.; Vimont, A.; Bedard, R.; Abdo, S.; Bricker, J., Zeolites in a Good Shape: Catalyst Forming by Extrusion Modifies their Performances, *Microporous Mesoporous Mater.* **2020**, *299*, 110114.
(103) Hafner, J.; Benco, L.; Bucko, T., Acid-Based Catalysis in Zeolites Investigated by Density-Functional Methods, *Topics Catal.* **2006**, *37*, 41-54.
(104) Van Speybroeck, V.; De Wispelaere, K.; Van der Mynsbrugge, J.; Vandichel, M.; Hemelsoet, K.; Waroquier, M., First Principle Chemical Kinetics in Zeolites: the Methanol-to-Olefin Process as a Case Study, *Chem. Soc. Rev.* **2014**, *43*, 7326-7357.

(105) Gubbins, K. E.; Liu, Y.-C.; Moore, J. D.; Palmer, J. C., The Role of Molecular Modeling in Confined Systems: Impact and Prospects, *Phys. Chem. Chem. Phys.* **2011**, *13*, 58-85.
(106) Li, G.; Pidko, E. A., The Nature and Catalytic Function of Cation Sites in Zeolites: a Computational Perspective, *ChemCatChem* **2018**, *11*, 134-156.
(107) Mansoor, E.; Van der Mynsbrugge, J.; Head-Gordon, M.; Bell, A. T., Impact of Long-Range Electrostatic and Dispersive Interactions on Theoretical Predictions of Adsorption and Catalysis in Zeolites, *Catal. Today* **2018**, *312*, 51-65.
(108) Sabbe, M. K.; Reyniers, M.-F.; Reuter, K., First-Principles Kinetic Modeling in Heterogeneous Catalysis: an Industrial Perspective on Best-Practice, Gaps and Needs, *Catal. Sci. Technol.* **2012**, *2*, 2010-2024.
(109) Chizallet, C.; Raybaud, P., Density Functional Theory Simulations of Complex Catalytic Materials in Reactive Environments: Beyond the Ideal Surface at Low Coverage, *Catal. Sci. Technol.* **2014**, *4*, 2797-2813.
(110) Pidko, E. A., Toward the Balance between the Reductionist and Systems Approaches in Computational Catalysis: Model versus Method Accuracy for the Description of Catalytic Systems, *ACS Catal.* **2017**, *7*, 4230-4234.
(111) Groen, J. C.; Bach, T.; Ziese, U.; Paulaime-van Donk, A. M.; de Jong, K. P.; Moulijn, J. A.; Perez-Ramirez, J., Creation of Hollow Zeolite Architectures by Controlled Desilication of Al-Zoned ZSM-5 Crystals, *J. Am. Chem. Soc.* **2005**, *127*, 10792-10793.
(112) Catlow, R.; Bell, R.; Cora, F.; Slater, B.,Chapter 19 - Molecular Modelling in Zeolite Science, In *Stud. Surf. Sci. Catal.*; Čejka, J., van Bekkum, H., Corma, A., Schüth, F., Eds.; Elsevier: 2007; Vol. 168, p 659-700.
(113) Bucko, T.; Benco, L.; Dubay, O.; Dellago, C.; Hafner, J., Mechanism of Alkane Dehydrogenation Catalyzed by Acidic Zeolites: Ab Initio Transition Path Sampling, *J. Chem. Phys.* **2009**, *131*, 214508.
(114) Bučko, T.; Benco, L.; Hafner, J.; Ángyán, J. G., Monomolecular Cracking of Propane over Acidic Chabazite: An Ab Initio Molecular Dynamics and Transition Path Sampling Study, *J. Catal.* **2011**, *279*, 220-228.
(115) Bucko, T.; Hafner, J., Entropy Effects in Hydrocarbon Conversion Reactions: Free-Energy Integrations and Transition-Path Sampling, *J. Phys.: Condens. Matter* **2010**, *22*, 384201.
(116) Rey, J.; Raybaud, P.; Chizallet, C.; Bučko, T., Competition of Secondary versus Tertiary Carbenium Routes for the Type B Isomerization of Alkenes over Acid Zeolites Quantified by Ab Initio Molecular Dynamics Simulations, *ACS Catal.* **2019**, *9*, 9813-9828.
(117) Rey, J.; Gomez, A.; Raybaud, P.; Chizallet, C.; Bučko, T., On the Origin of the Difference between Type A and Type B Skeletal Isomerization of Alkenes Catalyzed by Zeolites: The Crucial Input of Ab Initio Molecular Dynamics, *J. Catal.* **2019**, *373*, 361-373.
(118) Bučko, T.; Hafner, J., The Role of Spatial Constraints and Entropy in the Adsorption and Transformation of Hydrocarbons Catalyzed by Zeolites, *J. Catal.* **2015**, *329*, 32-48.
(119) Nielsen, M.; Hafreager, A.; Brogaard, R. Y.; De Wispelaere, K.; Falsig, H.; Beato, P.; Van Speybroeck, V.; Svelle, S., Collective Action of Water Molecules in Zeolite Dealumination, *Catal. Sci. Technol.* **2019**, *9*, 3721-3725.
(120) Cnudde, P.; De Wispelaere, K.; Vanduyfhuys, L.; Demuynck, R.; Van der Mynsbrugge, J.; Waroquier, M.; Van Speybroeck, V., How Chain Length and Branching Influence the Alkene Cracking Reactivity on H-ZSM-5, *ACS Catal.* **2018**, *8*, 9579-9595.
(121) Cnudde, P.; De Wispelaere, K.; Van der Mynsbrugge, J.; Waroquier, M.; Van Speybroeck, V., Effect of Temperature and Branching on the Nature and Stability of Alkene Cracking Intermediates in H-ZSM-5, *J. Catal.* **2017**, *345*, 53-69.
(122) Hajek, J.; Van der Mynsbrugge, J.; De Wispelaere, K.; Cnudde, P.; Vanduyfhuys, L.; Waroquier, M.; Van Speybroeck, V., On the Stability and Nature of Adsorbed Pentene in Brønsted Acid Zeolite H-ZSM-5 at 323K, *J. Catal.* **2016**, *340*, 227-235.
(123) Moors, S. L. C.; De Wispelaere, K.; Van der Mynsbrugge, J.; Waroquier, M.; Van Speybroeck, V., Molecular Dynamics Kinetic Study on the Zeolite-Catalyzed Benzene Methylation in ZSM-5, *ACS Catal.* **2013**, *3*, 2556-2567.
(124) De Wispelaere, K.; Bailleul, S.; Van Speybroeck, V., Towards Molecular Control of Elementary Reactions in Zeolite Catalysis by Advanced Molecular Simulations Mimicking Operating Conditions, *Catal. Sci. Technol.* **2016**, *6*, 2686-2705.

(125) Collins, G. A. D.; Cruickshank, D. W. J.; Breeze, A., Ab Initio Calculations on the Silicate Ion, Orthosilicic Acid and Their L2,3 X-Ray Spectra, *J. Chem. Soc., Faraday Trans. 2* **1972**, *68*, 1189-1195.
(126) Sauer, J.; Ŀurawski, B., Molecular and Electronic Structure of Disiloxane, an Ab Initio MO Study, *Chem. Phys. Lett.* **1979**, *65*, 587-591.
(127) Gibbs, G. V., Molecules as Models for Bonding in Silicates, *Am. Mineral.* **1982**, *67*, 421-450.
(128) Zhidomirov, G. M.; Kazansky, V. B., Quantum-Chemical Cluster Models of Acid-Base Sites of Oxide-Catalysts, *Adv. Catal.* **1986**, *34*, 131-202.
(129) White, J. C.; Hess, A. C., Periodic Hartree-Fock Study of Siliceous Mordenite, *J. Phys. Chem.* **1993**, *97*, 6398-6404.
(130) Nicholas, J. B.; Hess, A. C., Ab Initio Periodic Hartree-Fock Investigation of a Zeolite Acid Site, *J. Am. Chem. Soc.* **1994**, *116*, 5428-5436.
(131) Aprà, E.; Dovesi, R.; Freyria-Fava, C.; Pisani, C.; Roetti, C.; Saunders, V. R., Ab Initio Hartree-Fock Modelling of Zeolites: Application to Silico-Chabazite, *Model. Simul. Mater. Sci. Eng.* **1993**, *1*, 297-306.
(132) Campana, L.; Selloni, A.; Weber, J.; Pasquarello, A.; Papai, I.; Goursot, A., First Principles Molecular Dynamics Calculation of the Structure and Acidity of a Bulk Zeolite, *Chem. Phys. Lett.* **1994**, *226*, 245-250.
(133) Warshel, A.; Levitt, M., Theoretical Studies of Enzymic reactions: Dielectric, Electrostatic and Steric Stabilization of the Carbonium Ion in the Reaction of Lysozyme, *J. Mol. Biol.* **1976**, *103*, 227-249.
(134) Levitt, M., Birth and Future of Multiscale Modeling for Macromolecular Systems (Nobel Lecture), *Angew. Chem. Int. Ed.* **2014**, *53*, 10006-10018.
(135) Karplus, M., Development of Multiscale Models for Complex Chemical Systems: From $H+H_2$ to Biomolecules (Nobel Lecture), *Angew. Chem. Int. Ed.* **2014**, *53*, 9992-10005.
(136) Eichler, U.; Kölmel, C. M.; Sauer, J., Combining Ab Initio Techniques with Analytical Potential Functions for Structure Predictions of Large Systems: Method and Application to Crystalline Silica Polymorphs, *J. Comput. Chem.* **1997**, *18*, 463-477.
(137) Sauer, J.; Sierka, M., Combining Quantum Mechanics and Interatomic Potential Functions in Ab Initio Studies of Extended Systems, *J. Comput. Chem.* **2000**, *21*, 1470-1493.
(138) Sushko, P. V.; Gavartin, J. L.; Shluger, A. L., Electronic Properties of Structural Defects at the MgO (001) Surface, *J. Phys. Chem. B* **2002**, *106*, 2269-2276.
(139) de Jong, W. A.; Bylaska, E.; Govind, N.; Janssen, C. L.; Kowalski, K.; Muller, T.; Nielsen, I. M. B.; van Dam, H. J. J.; Veryazov, V.; Lindh, R., Utilizing High Performance Computing for Chemistry: Parallel Computational Chemistry, *Phys. Chem. Chem. Phys.* **2010**, *12*, 6896-6920.
(140) Tomasi, J.; Mennucci, B.; Cammi, R., Quantum Mechanical Continuum Solvation Models, *Chem. Rev.* **2005**, *105*, 2999-3094.
(141) Bulo, R. E.; Michel, C.; Fleurat-Lessard, P.; Sautet, P., Multiscale Modeling of Chemistry in Water: Are We There Yet?, *J Chem Theory Comput* **2013**, *9*, 5567-5577.
(142) Han, O. H.; Kim, C. S.; Hong, S. B., Direct Evidence for the Nonrandom Nature of Al Substitution in Zeolite ZSM-5: An Investigation by ^{27}Al MAS and MQ MAS NMR, *Angew. Chem. Int. Ed.* **2002**, *41*, 469-472.
(143) Sklenak, S.; Dedecek, J.; Li, C.; Wichterlova, B.; Gabova, V.; Sierka, M.; Sauer, J., Aluminum Siting in Silicon-Rich Zeolite Frameworks: A Combined High-Resolution ^{27}Al NMR Spectroscopy and Quantum Mechanics/Molecular Mechanics Study of ZSM-5, *Angew. Chem., Int. Ed* **2007**, *46*, 7286-7289.
(144) Dědeček, J.; Sobalík, Z.; Wichterlová, B., Siting and Distribution of Framework Aluminium Atoms in Silicon-Rich Zeolites and Impact on Catalysis, *Catal. Rev.* **2012**, *54*, 135-223.
(145) Holzinger, J.; Nielsen, M.; Beato, P.; Brogaard, R. Y.; Buono, C.; Dyballa, M.; Falsig, H.; Skibsted, J.; Svelle, S., Identification of Distinct Framework Aluminum Sites in Zeolite ZSM-23: A Combined Computational and Experimental ^{27}Al NMR Study, *J. Phys. Chem. C* **2018**, *123*, 7831-7844.
(146) Holzinger, J.; Beato, P.; Lundegaard, L. F.; Skibsted, J., Distribution of Aluminum over the Tetrahedral Sites in ZSM-5 Zeolites and Their Evolution after Steam Treatment, *J. Phys. Chem. C* **2018**, *122*, 15595-15613.

(147) van Bokhoven, J. A.; Lee, T. L.; Drakopoulos, M.; Lamberti, C.; Thieb, S.; Zegenhagen, J., Determining the Aluminium Occupancy on the Active T-Sites in Zeolites using X-Ray Standing Waves, *Nat. Mater.* **2008**, *7*, 551-555.
(148) Sarv, P.; Fernandez, C.; Amoureux, J.-P.; Keskinen, K., Distribution of Tetrahedral Aluminium Sites in ZSM-5 Type Zeolites: An ^{27}Al (Multiquantum) Magic Angle Spinning NMR Study, *J. Phys. Chem.* **1996**, *100*, 19223-19226.
(149) Sklenak, S.; Dědeček, J.; Li, C.; Wichterlová, B.; Gábová, V.; Sierka, M.; Sauer, J., Aluminium Siting in the ZSM-5 Framework by Combination of High Resolution ^{27}Al NMR and DFT/MM calculations, *Phys. Chem. Chem. Phys.* **2009**, *11*, 1237-1247.
(150) Dědeček, J.; Sklenak, S.; Li, C.; Wichterlová, B.; Gábová, V.; Brus, J.; Sierka, M.; Sauer, J., Effect of Al−Si−Al and Al−Si−Si−Al Pairs in the ZSM-5 Zeolite Framework on the ^{27}Al NMR Spectra. A Combined High-Resolution ^{27}Al NMR and DFT/MM Study, *J. Phys. Chem. C* **2009**, *113*, 1447-1458.
(151) Sarv, P.; Wichterlová, B.; Čejka, J., Multinuclear MQMAS NMR Study of NH_4/Na-Ferrierites, *J. Phys. Chem. B* **1998**, *102*, 1372-1378.
(152) Pinar, A. B.; Verel, R.; Pérez-Pariente, J.; van Bokhoven, J. A., Direct Evidence of the Effect of Synthesis Conditions on Aluminum Siting in Zeolite Ferrierite: A ^{27}Al MQ MAS NMR Study, *Microporous Mesoporous Mater.* **2014**, *193*, 111-114.
(153) van Bokhoven, J. A.; Koningsberger, D. C.; Kunkeler, P.; van Bekkum, H.; Kentgens, A. P. M., Stepwise Dealumination of Zeolite Beta at Specific T-Sites Observed with ^{27}Al MAS and ^{27}Al MQ MAS NMR, *J. Am. Chem. Soc.* **2000**, *122*, 12842-12847.
(154) Abraham, A.; Lee, S.-H.; Shin, C.-H.; Bong Hong, S.; Prins, R.; van Bokhoven, J. A., Influence of Framework Silicon to Aluminium Ratio on Aluminium Coordination and Distribution in Zeolite Beta Investigated by ^{27}Al MAS and ^{27}Al MQ MAS NMR, *Phys. Chem. Chem. Phys.* **2004**, *6*, 3031-3036.
(155) Hu, J. Z.; Wan, C.; Vjunov, A.; Wang, M.; Zhao, Z.; Hu, M. Y.; Camaioni, D. M.; Lercher, J. A., ^{27}Al MAS NMR Studies of HBEA Zeolite at Low to High Magnetic Fields, *J. Phys. Chem. C* **2017**, *121*, 12849-12854.
(156) Dědeček, J.; Sklenak, S.; Li, C.; Gao, F.; Brus, J.; Zhu, Q.; Tatsumi, T., Effect of Al/Si Substitutions and Silanol Nests on the Local Geometry of Si and Al Framework Sites in Silicone-Rich Zeolites: A Combined High Resolution ^{27}Al and ^{29}Si NMR and Density Functional Theory/Molecular Mechanics Study, *J. Phys. Chem. C* **2009**, *113*, 14454-14466.
(157) Sastre, G.; Fornes, V.; Corma, A., Preferential Siting of Bridging Hydroxyls and Their Different Acid Strengths in the Two-Channel System of MCM-22 Zeolite, *J. Phys. Chem. B* **2000**, *104*, 4349-4354.
(158) Sastre, G.; Fornes, V.; Corma, A., On the Preferential Location of Al and Proton Siting in Zeolites: A Computational and Infrared Study, *J. Phys. Chem. B* **2002**, *106*, 701-708.
(159) Wang, S.; He, Y.; Jiao, W.; Wang, J.; Fan, W., Recent Experimental and Theoretical Studies on Al Siting/Acid Site Distribution in Zeolite Framework, *Curr. Opin. Chem. Eng.* **2019**, *23*, 146-154.
(160) Muraoka, K.; Chaikittisilp, W.; Okubo, T., Energy Analysis of Aluminosilicate Zeolites with Comprehensive Ranges of Framework Topologies, Chemical Compositions, and Aluminum Distributions, *J. Am. Chem. Soc.* **2016**, *138*, 6184-6193.
(161) Schröder, K.-P.; Sauer, J.; Leslie, M.; A.Catlow, C. R., Siting of AI and Bridging Hydroxyl Groups in ZSM-5: A Computer Simulation Study, *Zeolites* **1992**, *12*, 20-23.
(162) Zhai, D.; Liu, Y.; Zheng, H.; Zhao, L.; Gao, J.; Xu, C.; Shen, B., A First-Principles Evaluation of the Stability, Accessibility, and Strength of Brønsted Acid Sites in Zeolites, *J. Catal.* **2017**, *352*, 627-637.
(163) Li, C.; Vidal-Moya, A.; Miguel, P. J.; Dedecek, J.; Boronat, M.; Corma, A., Selective Introduction of Acid Sites in Different Confined Positions in ZSM-5 and Its Catalytic Implications, *ACS Catal.* **2018**, *8*, 7688-7697.
(164) Dib, E.; Mineva, T.; Gaveau, P.; Véron, E.; Sarou-Kanian, V.; Fayon, F.; Alonso, B., Probing Disorder in Al-ZSM-5 Zeolites by ^{14}N NMR Spectroscopy, *J. Phys. Chem. C* **2017**, *121*, 15831-15841.

(165) Knott, B. C.; Nimlos, C. T.; Robichaud, D. J.; Nimlos, M. R.; Kim, S.; Gounder, R., Consideration of the Aluminum Distribution in Zeolites in Theoretical and Experimental Catalysis Research, *ACS Catal.* **2017**, *8*, 770-784.
(166) Demuth, T.; Hafner, J.; Benco, L.; Toulhoat, H., Structural and Acidic Properties of Mordenite. An ab Initio Density-Functional Study, *J. Phys. Chem. B* **2000**, *104*, 4593-4607.
(167) Gutierrez-Acebo, E.; Rey, J.; Bouchy, C.; Schuurman, Y.; Chizallet, C., Location of the Active Sites for Ethylcyclohexane Hydroisomerization by Ring Contraction and Expansion in the EUO Zeolitic Framework, *ACS Catal.* **2019**, *9*, 1692-1704.
(168) Ghorbanpour, A.; Rimer, J. D.; Grabow, L. C., Periodic, vdW-Corrected Density Functional Theory Investigation of the Effect of Al Siting in H-ZSM-5 on Chemisorption Properties and Site-Specific Acidity, *Catal. Comm.* **2014**, *52*, 98-102.
(169) Shi, L.; Yang, J.; Shen, G.; Zhao, Y.; Chen, R.; Shen, M.; Wen, Y.; Shan, B., The Influence of Adjacent Al Atoms on the Hydrothermal Stability of H-SSZ-13: a First-Principles Study, *Phys. Chem. Chem. Phys.* **2020**, *22*, 2930-2937.
(170) Göltl, F.; Love, A. M.; Schuenzel, S. C.; Wolf, P.; Mavrikakis, M.; Hermans, I., Computational Description of Key Spectroscopic Features of Zeolite SSZ-13, *Phys. Chem. Chem. Phys.* **2019**, *21*, 19065-19075.
(171) Wang, M.; Jaegers, N. R.; Lee, M. S.; Wan, C.; Hu, J. Z.; Shi, H.; Mei, D.; Burton, S. D.; Camaioni, D. M.; Gutierrez, O. Y.; Glezakou, V. A.; Rousseau, R.; Wang, Y.; Lercher, J. A., Genesis and Stability of Hydronium Ions in Zeolite Channels, *J. Am. Chem. Soc.* **2019**, *141*, 3444-3455.
(172) Losch, P.; Joshi, H. R.; Vozniuk, O.; Grunert, A.; Ochoa-Hernandez, C.; Jabraoui, H.; Badawi, M.; Schmidt, W., Proton Mobility, Intrinsic Acid Strength and Acid Site Location in Zeolites Revealed by VTIR and DFT Studies, *J. Am. Chem. Soc.* **2018**.
(173) Nusterer, E.; Blöchl, P. E.; Schwarz, K., Interaction of Water and Methanol with a Zeolite at High Coverages, *Chem. Phys. Lett.* **1996**, *253*, 448-455.
(174) Benco, Ľ.; Demuth, T.; Hafner, J.; Hutschka, F., Spontaneous Proton Transfer between O-Sites in Zeolites, *Chem. Phys. Lett.* **2000**, *324*, 373-380.
(175) Li, X.-Z.; Walker, B.; Michaelides, A., Quantum Nature of the Hydrogen Bond, *Proceedings of the National Academy of Sciences* **2011**, *108*, 6369.
(176) Wilkins, D. M.; Manolopoulos, D. E.; Pipolo, S.; Laage, D.; Hynes, J. T., Nuclear Quantum Effects in Water Reorientation and Hydrogen-Bond Dynamics, *J Phys Chem Lett* **2017**, *8*, 2602-2607.
(177) Hibbs, A.; Feynman, R. P. *Quantum Mechanics and Path Integrals*; McGraw-Hill Interamericana, 1965.
(178) Ceriotti, M.; Manolopoulos, D. E.; Parrinello, M., Accelerating the Convergence of Path Integral Dynamics with a Generalized Langevin Equation, *J. Chem. Phys.* **2011**, *134*, 084104.
(179) Schröder, K. P.; Sauer, J.; Leslie, M.; Catlow, C. R. A.; Thomas, J. M., Bridging Hydroxyl Groups in Zeolitic Catalysts: a Computer Simulation of their Structure, Vibrational Properties and Acidity in Protonated Faujasites (H-Y Zeolites), *Chem. Phys. Lett.* **1992**, *188*, 320-325.
(180) Brand, H. V.; Curtiss, L. A.; Iton, L. E., Computational Studies of Acid Sites in ZSM 5: Dependence on Cluster Size, *J. Phys. Chem.* **1992**, *96*, 7725-7732.
(181) Brand, H. V.; Curtiss, L. A.; Iton, L. E., Ab Initio Molecular Orbital Cluster Studies of the Zeolite ZSM-5. 1. Proton Affinities, *J. Phys. Chem.* **1993**, *97*, 12773-12782.
(182) Redondo, A.; Hay, P. J., Quantum Chemical Studies of Acid Sites in Zeolite ZSM-5, *J. Phys. Chem.* **1993**, *97*, 11754-11761.
(183) Eichler, U.; Brändle, M.; Sauer, J., Predicting Absolute and Site Specific Acidities for Zeolite Catalysts by a Combined Quantum Mechanics/Interatomic Potential Function Approach, *J. Phys. Chem. B* **1997**, *101*, 10035-10050.
(184) Rybicki, M.; Sauer, J., Acid Strength of Zeolitic Brønsted Sites—Dependence on Dielectric Properties, *Catal. Today* **2019**, *323*, 86-93.
(185) Jones, A. J.; Iglesia, E., The Strength of Brønsted Acid Sites in Microporous Aluminosilicates, *ACS Catal.* **2015**, *5*, 5741-5755.
(186) Knözinger, H.,Infrared Spectroscopy for the Characterization of Surface Acidity and Basicity, In *Handbook of Heterogeneous Catalysis*; Ertl, G., Knözinger, H., Weitkamp, J., Eds.; Wiley: Weinheim, 1997; Vol. 2, p 707-732.

(187) Boronat, M.; Corma, A., What Is Measured When Measuring Acidity in Zeolites with Probe Molecules?, *ACS Catal.* **2019**, *9*, 1539-1548.
(188) Göltl, F.; Grüneis, A.; Bucko, T.; Hafner, J., Van der Waals Interactions Between Hydrocarbon Molecules and Zeolites: Periodic Calculations at Different Levels of Theory, from Density Functional Theory to the Random Phase Approximation and Møller-Plesset Perturbation Theory, *J. Chem. Phys.* **2012**, *137*, 114111.
(189) Piccini, G.; Alessio, M.; Sauer, J.; Zhi, Y.; Liu, Y.; Kolvenbach, R.; Jentys, A.; Lercher, J. A., Accurate Adsorption Thermodynamics of Small Alkanes in Zeolites. Ab initio Theory and Experiment for H-Chabazite, *J. Phys. Chem. C* **2015**, *119*, 6128-6137.
(190) Kazansky, V. B.; Senchenya, I. N., Quantum Chemical Study of the Electronic Structure and Geometry of Surface Alkoxy Groups as Probable Active Intermediates of Heterogeneous Acidic Catalysts: What Are the Adsorbed Carbenium Ions?, *J. Catal.* **1989**, *119*, 108-120.
(191) Viruela-Martin, P.; Zicovich-Wilson, C. M.; Corma, A., Ab Initio Molecular Orbital Calculations of the Protonation Reaction of Propylene and Isobutene by Acidic OH Groups of Isomorpbously Substituted Zeolites, *J. Phys. Chem.* **1993**, *97*, 13713-13719.
(192) Kazansky, V. B.; Frash, M. V.; van Santen, R. A., Quantumchemical Study of the Isobutane Cracking on Zeolites, *Appl. Catal. A* **1996**, *146*, 225-247.
(193) Hay, J. P.; Redondo, A.; Guo, Y., Theoretical Studies of Pentene Cracking on Zeolites: C–C β-Scission Processes, *Catal. Today* **1999**, *50*, 517-523.
(194) Rozanska, X.; van Santen, R.; Hutschka, F.; Hafner, J., A Periodic DFT Study of Intramolecular Isomerization Reactions of Toluene and Xylenes Catalyzed by Acidic Mordenite, *J. Am. Chem. Soc.* **2001**, *123*, 7655-7667.
(195) Benco, L.; Hafner, J.; Hutschka, F.; Toulhoat, H., Physisorption and Chemisorption of Some n-Hydrocarbons at the Brønsted Acid Site in Zeolites 12-Membered Ring Main Channels: Ab Initio Study of the Gmelinite Structure, *J. Phys. Chem. B* **2003**, *107*, 9756-9762.
(196) Boronat, M.; Viruela, P. M.; Corma, A., Reaction Intermediates in Acid Catalysis by Zeolites: Prediction of the Relative Tendency To Form Alkoxides or Carbocations as a Function of Hydrocarbon Nature and Active Site Structure, *J. Am. Chem. Soc.* **2004**, *126*, 3300-3309.
(197) Tuma, C.; Sauer, J., Protonated Isobutene in Zeolites: tert-Butyl Cation or Alkoxide?, *Angew. Chem. Int. Ed.* **2005**, *44*, 4769-4771.
(198) Tuma, C.; Kerber, T.; Sauer, J., The tert-Butyl Cation in H-Zeolites: Deprotonation to Isobutene and Conversion into Surface Alkoxides, *Angew. Chem. Int. Ed.* **2010**, *49*, 4678-4680.
(199) Fang, H.; Zheng, A.; Xu, J.; Li, S.; Chu, Y.; Chen, L.; Deng, F., Theoretical Investigation of the Effects of the Zeolite Framework on the Stability of Carbenium Ions, *J. Phys. Chem. C* **2011**, *115*, 7429-7439.
(200) Svelle, S.; Tuma, C.; Rozanska, X.; Kerber, T.; Sauer, J., Quantum Chemical Modeling of Zeolite-Catalyzed Methylation Reactions: Toward Chemical Accuracy for Barriers, *J. Am. Chem. Soc.* **2009**, *131*, 816-825.
(201) Piccini, G.; Alessio, M.; Sauer, J., Ab Initio Calculation of Rate Constants for Molecule–Surface Reactions with Chemical Accuracy, *Angew. Chem. Int. Ed.* **2016**, *55*, 5235-5237.
(202) Rybicki, M.; Sauer, J., Ab Initio Prediction of Proton Exchange Barriers for Alkanes at Brønsted Sites of Zeolite H-MFI, *J. Am. Chem. Soc.* **2018**, *140*, 18151−18161.
(203) Plessow, P. N.; Studt, F., Olefin Methylation and Cracking Reactions in H-SSZ-13 Investigated with Ab Initio and DFT Calculations, *Catal. Sci. Technol.* **2018**, *8*, 4420-4429.
(204) Blaszkowski, S. R.; van Santen, R. A., The Mechanism of Dimethyl Ether Formation from Methanol Catalyzed by Zeolitic Protons, *J. Am. Chem. Soc.* **1996**, *118*, 5152-5153.
(205) Blaszkowski, S. R.; van Santen, R. A., Theoretical Study of the Mechanism of Surface Methoxy and Dimethyl Ether Formation from Methanol Catalyzed by Zeolitic Protons, *J. Am. Chem. Soc.* **1997**, *101*, 2292-2305.
(206) Konda, S. S. M.; Caratzoulas, S.; Vlachos, D. G., Computational Insights into the Role of Metal and Acid Sites in Bifunctional Metal/Zeolite Catalysts: A Case Study of Acetone Hydrogenation to 2-Propanol and Subsequent Dehydration to Propene, *ACS Catal.* **2016**, *6*, 123-133.
(207) Zhi, Y.; Shi, H.; Mu, L.; Liu, Y.; Mei, D.; Camaioni, D. M.; Lercher, J. A., Dehydration Pathways of 1-Propanol on HZSM-5 in the Presence and Absence of Water, *J. Am. Chem. Soc.* **2015**, *137*, 15781-15794.

(208) Kim, S.; Robichaud, D. J.; Beckham, G. T.; Paton, R. S.; Nimlos, M. R., Ethanol Dehydration in HZSM-5 Studied by Density Functional Theory: Evidence for a Concerted Process, *J. Phys. Chem. A* **2015**, *119*, 3604-3614.
(209) John, M.; Alexopoulos, K.; Reyniers, M.-F.; Marin, G. B., Reaction Path Analysis for 1-Butanol Dehydration in H-ZSM-5 Zeolite: Ab Initio and Microkinetic Modeling, *J. Catal.* **2015**, *330*, 28-45.
(210) John, M.; Alexopoulos, K.; Reyniers, M.-F.; Marin, G. B., First-Principles Kinetic Study on the Effect of the Zeolite Framework on 1-Butanol Dehydration, *ACS Catal.* **2016**, *6*, 4081-4094.
(211) John, M.; Alexopoulos, K.; Reyniers, M.-F.; Marin, G. B., Mechanistic Insights into the Formation of Butene Isomers from 1-Butanol in H-ZSM-5: DFT based Microkinetic Modelling, *Catal. Sci. Technol.* **2017**, *7*, 1055-1072.
(212) John, M.; Alexopoulos, K.; Reyniers, M.-F.; Marin, G. B., Effect of Zeolite Confinement on the Conversion of 1-Butanol to Butene Isomers: Mechanistic Insights from DFT Based Microkinetic Modelling, *Catal. Sci. Technol.* **2017**, *7*, 2978-2997.
(213) Plessow, P. N.; Smith, A.; Tischer, S.; Studt, F., Identification of the Reaction Sequence of the MTO Initiation Mechanism Using Ab Initio-Based Kinetics, *J. Am. Chem. Soc.* **2019**, *141*, 5908-5915.
(214) Sabbe, M. K.; Canduela-Rodriguez, G.; Joly, J.-F.; Reyniers, M.-F.; Marin, G. B., Ab Initio Coverage-Dependent Microkinetic Modeling of Benzene Hydrogenation on Pd(111), *Catal. Sci. Technol.* **2017**, *7*, 5267-5283.
(215) Liu, C.; van Santen, R. A.; Poursaeidesfahani, A.; Vlugt, T. J. H.; Pidko, E. A.; Hensen, E. J. M., Hydride Transfer versus Deprotonation Kinetics in the Isobutane-Propene Alkylation Reaction: A Computational Study, *ACS Catal* **2017**, *7*, 8613-8627.
(216) Ruiz, J. M.; McAdon, M. H.; Garcés, J. M., Aluminum Complexes as Models for Broensted Acid Sites in Zeolites: Structure and Energetics of $[Al(OH)_4]^-$, $[Al(H_2O)_6]^{3+}$, and Intermediate Monomeric Species $[Al(OH)_x(H_2O)_{n-x}\cdot mH_2O]^{3-x}$ Obtained by Hydrolysis, *J. Phys. Chem. B* **1997**, *101*, 1733-1744.
(217) Benco, L.; Demuth, T.; Hafner, J.; Kutschka, F.; Toulhoat, H., Extraframework Aluminum Species in Zeolites: Ab Initio Molecular Dynamics Simulation of Gmelinite, *J. Catal.* **2002**, *209*, 480-488.
(218) Bhering, D. L.; Ramirez-Solis, A.; Mota, C. J. A., A Density Functional Theory Based Approach to Extraframework Aluminum Species in Zeolites, *J. Phys. Chem. B* **2003**, *107*, 4342-4347.
(219) Li, S.; Zheng, A.; Su, Y.; Fang, H.; Shen, W.; Yu, Z.; Chen, L.; Deng, F., Extra-Framework Aluminium Species in Hydrated Faujasite Zeolite as Investigated by Two-Dimensional Solid-State NMR Spectroscopy and Theoretical Calculations, *Phys. Chem. Chem. Phys.* **2010**, *12*, 3895-3903.
(220) Benco, L.; Bucko, T.; Hafner, J.; Toulhoat, H., Ab Initio Simulation of Lewis Sites in Mordenite and Comparative Study of the Strength of Active Sites via CO Adsorption, *J. Phys. Chem. B* **2004**, *108*, 13656-13666.
(221) Liu, C.; Li, G.; Hensen, E. J. M.; Pidko, E. A., Nature and Catalytic Role of Extraframework Aluminum in Faujasite Zeolite: A Theoretical Perspective, *ACS Catal.* **2015**, *5*, 7024-7033.
(222) Liu, C.; Li, G.; Hensen, E. J. M.; Pidko, E. A., Relationship Between Acidity and Catalytic Reactivity of Faujasite Zeolite: A Periodic DFT Study, *J. Catal.* **2016**, *344*, 570-577.
(223) Silaghi, M.-C.; Chizallet, C.; Sauer, J.; Raybaud, P., Dealumination Mechanisms of Zeolites and Extra-Framework Aluminum Confinement, *J. Catal.* **2016**, *339*, 242-255.
(224) Mirodatos, C.; Barthomeuf, D., Superacid Sites in Zeolites, *J. Chem. Soc., Chem. Commun.* **1981**, 39-40.
(225) Mota, C. J. A.; Bhering, D. L.; Rosenbach, N., A DFT Study of the Acidity of Ultrastable Y Zeolite: Where Is the Brønsted/Lewis Acid Synergism?, *Angew. Chem. Int. Ed.* **2004**, *43*, 3050-3053.
(226) Rosenbach, N.; Mota, C. J. A., A DFT–ONIOM Study on the Effect of Extra-Framework Aluminum on USY Zeolite Acidity, *Appl. Catal. A* **2008**, *336*, 54-60.
(227) Li, S.; Zheng, A.; Su, Y.; Zhang, H.; Yang, J.; Ye, C.; Deng, F., Brønsted/Lewis Acid Synergy in Dealuminated HY Zeolite: A Combined Solid-State NMR and Theoretical Calculation Study, *J. Am. Chem. Soc.* **2007**, *129*, 11161-11171.

(228) Yi, X.; Liu, K.; Chen, W.; Li, J.; Xu, S.; Li, C.; Xiao, Y.; Liu, H.; Guo, X.; Liu, S. B.; Zheng, A., Origin and Structural Characteristics of Tri-coordinated Extra-framework Aluminum Species in Dealuminated Zeolites, *J. Am. Chem. Soc.* **2018**, *140*, 10764-10774.
(229) Bordiga, S.; Ugliengo, P.; Damin, A.; Lamberti, C.; Spoto, G.; Zecchina, A.; Spano, G.; Buzzoni, R.; Dalloro, L.; Rivetti, F., Hydroxyls Nests in Defective Silicalites and Strained Structures Derived upon Dehydroxylation: Vibrational Properties and Theoretical Modelling, *Topics Catal.* **2001**, *15*, 43-52.
(230) Dědeček, J. i.; Sklenak, S.; Li, C.; Gao, F.; Brus, J. i.; Zhu, Q.; Tatsumi, T., Effect of Al/Si Substitutions and Silanol Nests on the Local Geometry of Si and Al Framework Sites in Silicone-Rich Zeolites: A Combined High Resolution 27 Al and 29 Si NMR and Density Functional Theory/Molecular Mechanics Study, *J. Phys. Chem. C* **2009**, *113*, 14454-14466.
(231) Catlow, C. R. A.; Baram, P. S.; Parker, S. C.; Purton, J.; Wright, K. V., Protons in Oxides, *Radiat. Eff. Defects Solids* **1995**, *134*, 57-64.
(232) Sokol, A. A.; Catlow, C. R. A.; Garces, J. M.; Kuperman, A., Defect Centers in Microporous Aluminum Silicate Materials, *J. Phys. Chem. B* **1998**, *102*, 10647-10649.
(233) Sokol, A. A.; Catlow, C. R. A.; Garces, J. M.; Kuperman, A., Computational Investigation into the Origins of Lewis Acidity in Zeolites, *Adv. Mater.* **2000**, *12*, 1801-1805.
(234) Sokol, A. A.; Catlow, C. R. A.; Garcés, J. M.; Kuperman, A., Local States in Microporous Silica and Aluminum Silicate Materials. 1. Modeling Structure, Formation, and Transformation of Common Hydrogen Containing Defects, *J. Phys. Chem. B* **2002**, *106*, 6163-6177.
(235) Sokol, A. A.; Catlow, C. R. A.; Garcés, J. M.; Kuperman, A., Transformation of Hydroxyl Nests in Microporous Aluminosilicates upon Annealing, *J. Phys.: Condens. Matter* **2004**, *16*, S2781-S2794.
(236) Senderov, E.; Halasz, I.; Olson, D. H., On Existence of Hydroxyl Nests in Acid Dealuminated Zeolite Y, *Microporous Mesoporous Mater.* **2014**, *186*, 94-100.
(237) Halasz, I.; Senderov, E.; Olson, D. H.; Liang, J.-J., Further Search for Hydroxyl Nests in Acid Dealuminated Zeolite Y, *J. Phys. Chem. C* **2015**, *119*, 8619-8625.
(238) Lisboa, O.; Sánchez, M.; Ruette, F., Modeling Extra Framework Aluminum (EFAL) Formation in the Zeolite ZSM-5 Using Parametric Quantum and DFT Methods, *J. Mol. Catal. A* **2008**, *294*, 93-101.
(239) Malola, S.; Svelle, S.; Bleken, F. L.; Swang, O., Detailed Reaction Paths for Zeolite Dealumination and Desilication From Density Functional Calculations, *Angew. Chem. Int. Ed.* **2012**, *51*, 652-655.
(240) Fjermestad, T.; Svelle, S.; Swang, O., Desilication of SAPO-34: Reaction Mechanisms from Periodic DFT Calculations, *J. Phys. Chem. C* **2015**, *119*, 2073-2085.
(241) Silaghi, M.-C.; Chizallet, C.; Petracovschi, E.; Kerber, T.; Sauer, J.; Raybaud, P., Regioselectivity of Al-O Bond Hydrolysis During Zeolites Dealumination Unified by Brønsted-Evans-Polanyi Relationship, *ACS Catal.* **2015**, *5*, 11-15.
(242) Nielsen, M.; Brogaard, R. Y.; Falsig, H.; Beato, P.; Swang, O.; Svelle, S., Kinetics of Zeolite Dealumination: Insights from H-SSZ-13, *ACS Catal.* **2015**, *5*, 7131-7139.
(243) Valdiviés-Cruz, K.; Lam, A.; Zicovich-Wilson, C. M., Full Mechanism of Zeolite Dealumination in Aqueous Strong Acid Medium: Ab Initio Periodic Study on H-Clinoptilolite, *J. Phys. Chem. C* **2017**, *121*, 2652-2660.
(244) Sun, J.; Fang, H.; Ravikovitch, P. I.; Sholl, D. S., Understanding Dealumination Mechanisms in Protonic and Cationic Zeolites, *J. Phys. Chem. C* **2020**, *124*, 668-676.
(245) Louwen, J. N.; Simko, S.; Stanciakova, K.; Bulo, R. E.; Weckhuysen, B. M.; Vogt, E. T. C., Role of Rare Earth Ions in the Prevention of Dealumination of Zeolite Y for Fluid Cracking Catalysts, *J. Phys. Chem. C* **2020**, *124*, 4626-4636.
(246) Heard, C. J.; Grajciar, L.; Rice, C. M.; Pugh, S. M.; Nachtigall, P.; Ashbrook, S. E.; Morris, R. E., Fast Room Temperature Lability of Aluminosilicate Zeolites, *Nature Commun.* **2019**, *10*, 4690.
(247) Valdivies-Cruz, K.; Lam, A.; Zicovich-Wilson, C. M., Chemical Interaction of Water Molecules with Framework Al in Acid Zeolites: a Periodic Ab Initio Study on H-Clinoptilolite, *Phys. Chem. Chem. Phys.* **2015**, *17*, 23657-23666.

(248) Stanciakova, K.; Ensing, B.; Göltl, F.; Bulo, R. E.; Weckhuysen, B. M., Cooperative Role of Water Molecules during the Initial Stage of Water-Induced Zeolite Dealumination, *ACS Catal.* **2019**, *9*, 5119-5135.
(249) Ohsuna, T.; Slater, B.; Gao, F.; Yu, J.; Sakamoto, Y.; Zhu, G.; Terasaki, O.; Vaughan, D. E.; Qiu, S.; Catlow, C. R., Fine Structures of Zeolite-Linde-L (LTL): Surface Structures, Growth Unit and Defects, *Chemistry* **2004**, *10*, 5031-5040.
(250) Pitman, M. C.; van Duin, A. C., Dynamics of Confined Reactive Water in Smectite Clay-Zeolite Composites, *J. Am. Chem. Soc.* **2012**, *134*, 3042-3053.
(251) Bai, C.; Liu, L.; Sun, H., Molecular Dynamics Simulations of Methanol to Olefin Reactions in HZSM-5 Zeolite Using a ReaxFF Force Field, *J. Phys. Chem. C* **2012**, *116*, 7029-7039.
(252) Joshi, K. L.; van Duin, A. C. T., Molecular Dynamics Study on the Influence of Additives on the High-Temperature Structural and Acidic Properties of ZSM-5 Zeolite, *Energy Fuels* **2013**, *27*, 4481-4488.
(253) Joshi, K. L.; Psofogiannakis, G.; van Duin, A. C. T.; Raman, S., Reactive Molecular Simulations of Protonation of Water Clusters and Depletion of Acidity in H-ZSM-5 Zeolite, *Phys. Chem. Chem. Phys.* **2014**, *16*, 18433-18441.
(254) Prestianni, A.; Cortese, R.; Duca, D., Propan-2-ol Dehydration on H-ZSM-5 and H-Y Zeolite: a DFT Study, *React. Kinet. Catal.* **2013**, *108*, 565-582.
(255) Loades, S. D.; Carr, S. W.; Gay, D. H.; Rohl, A. L., Calculation of the Morphology of Silica Sodalite, *J. Chem. Soc., Chem. Commun.* **1994**, 1369-1370.
(256) Baram, P. S.; Parker, S. C., Atomistic Simulation of Hydroxide Ions in Inorganic Solids, *Philosophical Magazine B* **1996**, *73*, 49-58.
(257) Civalleri, B.; Casassa, S.; Garrone, E.; Pisani, C.; Ugliengo, P., Quantum Mechanical ab Initio Characterization of a Simple Periodic Model of the Silica Surface, *J. Phys. Chem. B* **1999**, *103*, 2165-2171.
(258) Bucko, T.; Benco, L.; Hafner, J., Defect Sites at the (001) Surface of Mordenite: An Ab Initio Study, *J. Chem. Phys.* **2003**, *118*, 8437-8445.
(259) Bucko, T.; Hafner, J.; Benco, L., Adsorption and Vibrational Spectroscopy of Ammonia at Mordenite: Ab Initio Study, *J. Chem. Phys.* **2004**, *120*, 10263-10277.
(260) Khalil, I.; Celis-Cornejo, C. M.; Thomas, K.; Bazin, P.; Travert, A.; Pérez-Martínez, D. J.; Baldovino-Medrano, V. G.; Paul, J. F.; Maugé, F., In Situ IR-ATR Study of the Interaction of Nitrogen Heteroaromatic Compounds with HY Zeolites: Experimental and Theoretical Approaches, *ChemCatChem* **2019**, *12*, 1095-1108.
(261) Stoyanov, S. R.; Gusarov, S.; Kuznicki, S. M.; Kovalenko, A., Theoretical Modeling of Zeolite Nanoparticle Surface Acidity for Heavy Oil Upgrading, *J. Phys. Chem. C* **2008**, *112*, 6794-6810.
(262) Slater, B.; Catlow, C. R. A.; Liu, Z.; Ohsuna, T.; Terasaki, O.; Camblor, M. A., Surface Structure and Crystal Growth of Zeolite Beta C, *Angew. Chem. Int. Ed.* **2002**, *41*, 1235-1237.
(263) Slater, B.; Titiloye, J. O.; Higgins, F. M.; Parker, S. C., Atomistic Simulation of Zeolite Surfaces, *Curr. Opin. Solid State Mater. Sci.* **2001**, *5*, 417-424.
(264) Abril, D. M.; Slater, B.; Blanco, C., Modeling Dynamics of the External Surface of Zeolite LTA, *Microporous Mesoporous Mater.* **2009**, *123*, 268-273.
(265) Greń, W.; Parker, S. C.; Slater, B.; Lewis, D. W., Structure of Zeolite A (LTA) Surfaces and the Zeolite A/Water Interface, *J. Phys. Chem. C* **2010**, *114*, 9739-9747.
(266) Hermann, J.; Trachta, M.; Nachtigall, P.; Bludský, O., Theoretical Investigation of Layered Zeolite Frameworks: Surface Properties of 2D Zeolites, *Catal. Today* **2014**, *227*, 2-8.
(267) Whitmore, L.; Slater, B.; Catlow, C. R. A., Adsorption of Benzene at the Hydroxylated (111) External Surface of Faujasite, *Phys. Chem. Chem. Phys.* **2000**, *2*, 5354-5356.
(268) Kubo, M.; Oumi, Y.; Takaba, H.; Chatterjee, A.; Miyamoto, A., Chemical Vapor Deposition Process on the ZSM-5(010) Surface as Investigated by Molecular Dynamics, *J. Phys. Chem. B* **1999**, *103*, 1876-1880.
(269) Ho, T. V.; Nachtigall, P.; Grajciar, L., The Lewis Acidity of Three- and Two-Dimensional Zeolites: The Effect of Framework Topology, *Catal. Today* **2018**, *304*, 12-21.
(270) Varoon, K.; Zhang, X.; Elyassi, B.; Brewer, D. D.; Gettel, M.; Kumar, S.; Lee, J. A.; Maheshwari, S.; Mittal, A.; Sung, C.-Y.; Cococcioni, M.; Francis, L. F.; McCormick, A. V.;

Mkhoyan, K. A.; Tsapatsis, M., Dispersible Exfoliated Zeolite Nanosheets and Their Application as a Selective Membrane, *Science* **2011**, *334*, 72.
(271) Thang, H. V.; Vaculík, J.; Přech, J.; Kubů, M.; Čejka, J.; Nachtigall, P.; Bulánek, R.; Grajciar, L., The Brønsted Acidity of Three- and Two-Dimensional Zeolites, *Microporous Mesoporous Mater.* **2019**, *282*, 121-132.
(272) Rybicki, M.; Sauer, J., Acidity of Two-Dimensional Zeolites, *Phys. Chem. Chem. Phys.* **2015**, *17*, 27873-27882.
(273) Boscoboinik, J. A.; Yu, X.; Yang, B.; Fischer, F. D.; Wlodarczyk, R.; Sierka, M.; Shaikhutdinov, S.; Sauer, J.; Freund, H. J., Modeling Zeolites with Metal-Supported Two-Dimensional Aluminosilicate Films, *Angew. Chem. Int. Ed.* **2012**, *51*, 6005-6008.
(274) Thang, H. V.; Rubes, M.; Bludsky, O.; Nachtigall, P., Computational Investigation of the Lewis Acidity in Three-Dimensional and Corresponding Two-Dimensional Zeolites: UTL vs IPC-1P, *J. Phys. Chem. A* **2014**, *118*, 7526-7534.
(275) Boscoboinik, J. A.; Yu, X.; Emmez, E.; Yang, B.; Shaikhutdinov, S.; Fischer, F. D.; Sauer, J.; Freund, H.-J., Interaction of Probe Molecules with Bridging Hydroxyls of Two-Dimensional Zeolites: A Surface Science Approach, *J. Phys. Chem. C* **2013**, *117*, 13547-13556.
(276) Witman, M.; Ling, S.; Boyd, P.; Barthel, S.; Haranczyk, M.; Slater, B.; Smit, B., Cutting Materials in Half: A Graph Theory Approach for Generating Crystal Surfaces and Its Prediction of 2D Zeolites, *ACS Cent. Sci.* **2018**, *4*, 235-245.
(277) Kirschhock, C. E. A.; Ravishankar, R.; Looveren, L. V.; Jacobs, P. A.; Martens, J. A., Mechanism of Transformation of Precursors into Nanoslabs in the Early Stages of MFI and MEL Zeolite Formation from TPAOH−TEOS−H_2O and TBAOH−TEOS−H_2O Mixtures, *J. Phys. Chem. B* **1999**, *103*, 4972-4978.
(278) Drake, I. J.; Zhang, Y.; Gilles, M. K.; Teris Liu, C. N.; Nachimuthu, P.; Perera, R. C. C.; Wakita, H.; Bell, A. T., An In Situ Al K-Edge XAS Investigation of the Local Environment of H^+- and Cu^+-Exchanged USY and ZSM-5 Zeolites, *J. Phys. Chem. B* **2006**, *110*, 11665-11676.
(279) Ravi, M.; Sushkevich, V. L.; van Bokhoven, J. A., Lewis Acidity Inherent to the Framework of Zeolite Mordenite, *J. Phys. Chem. C* **2019**, *123*, 15139-15144.
(280) Bucko, T.; Hafner, J.; Benco, L., Adsorption and Vibrational Spectroscopy of CO on Mordenite: Ab Initio Density-Functional Study, *J. Phys. Chem. B* **2005**, *109*, 7345-7357.
(281) Hernandez-Tamargo, C. E.; Roldan, A.; de Leeuw, N. H., DFT Modeling of the Adsorption of Trimethylphosphine Oxide at the Internal and External Surfaces of Zeolite MFI, *J. Phys. Chem. C* **2016**, *120*, 19097-19106.
(282) Leydier, F.; Chizallet, C.; Costa, D.; Raybaud, P., CO Adsorption on Amorphous Silica–Alumina: Electrostatic or Brønsted Acidity Probe?, *Chem. Commun.* **2012**, *48*, 4076-4078.
(283) Bucko, T.; Hafner, J.; Benco, L., Active Sites for the Vapor Phase Beckmann Rearrangement over Mordenite: An ab Initio Study, *J. Phys. Chem. A* **2004**, *108*, 11388-11397.
(284) Hernandez-Tamargo, C. E.; Roldan, A.; de Leeuw, N. H., Density Functional Theory Study of the Zeolite-Mediated Tautomerization of Phenol and Catechol, *Molecular Catalysis* **2017**, *433*, 334-345.
(285) Leydier, F.; Chizallet, C.; Costa, D.; Raybaud, P., Revisiting Carbenium Chemistry on Amorphous Silica-Alumina: Unraveling their Milder Acidity as Compared to Zeolites, *J. Catal.* **2015**, *325*, 35-47.
(286) Takaba, H.; Koyama, A.; Nakao, S.-i., Dual Ensemble Monte Carlo Simulation of Pervaporation of an Ethanol/Water Binary Mixture in Silicalite Membrane Based on a Lennard-Jones Interaction Model, *J. Phys. Chem. B* **2000**, *104*, 6353-6359.
(287) Schnell, S. K.; Wu, L.; Koekkoek, A. J. J.; Kjelstrup, S.; Hensen, E. J. M.; Vlugt, T. J. H., Adsorption of Argon on MFI Nanosheets: Experiments and Simulations, *J. Phys. Chem. C* **2013**, *117*, 24503-24510.
(288) Liu, Y.; Chen, X., High Permeability and Salt Rejection Reverse Osmosis by a Zeolite Nano-Membrane, *Phys. Chem. Chem. Phys.* **2013**, *15*, 6817-6824.
(289) Inzoli, I.; Simon, J.-M.; Kjelstrup, S., Surface Adsorption Isotherms and Surface Excess Densities of n-Butane in Silicalite-1, *Langmuir* **2009**, *25*, 1518-1525.
(290) García-Pérez, E.; Schnell, S. K.; Castillo, J. M.; Calero, S.; Kjelstrup, S.; Dubbeldam, D.; Vlugt, T. J. H., External Surface Adsorption on Silicalite-1 Zeolite Studied by Molecular Simulation, *J. Phys. Chem. C* **2011**, *115*, 15355-15360.

(291) Zimmermann, N. E. R.; Balaji, S. P.; Keil, F. J., Surface Barriers of Hydrocarbon Transport Triggered by Ideal Zeolite Structures, *J. Phys. Chem. C* **2012**, *116*, 3677-3683.
(292) Sastre, G.; Kärger, J.; Ruthven, D. M., Molecular Dynamics Study of Diffusion and Surface Permeation of Benzene in Silicalite, *J. Phys. Chem. C* **2018**, *122*, 7217-7225.
(293) Zimmermann, N. E. R.; Zabel, T. J.; Keil, F. J., Transport into Nanosheets: Diffusion Equations Put to Test, *J. Phys. Chem. C* **2013**, *117*, 7384-7390.
(294) Bai, P.; Haldoupis, E.; Dauenhauer, P. J.; Tsapatsis, M.; Siepmann, J. I., Understanding Diffusion in Hierarchical Zeolites with House-of-Cards Nanosheets, *ACS Nano* **2016**, *10*, 7612-7618.
(295) Mora-Fonz, M. J.; Catlow, C. R. A.; Lewis, D. W., Modeling Aqueous Silica Chemistry in Alkali Media, *J. Phys. Chem. C* **2007**, *111*, 18155-18158.
(296) Trinh, T. T.; Tran, K.-Q.; Zhang, X.-Q.; van Santen, R. A.; Meijer, E. J., The Role of a Structure Directing Agent Tetramethylammonium Template in the Initial Steps of Silicate Oligomerization in Aqueous Solution, *Phys. Chem. Chem. Phys.* **2015**, *17*, 21810-21818.
(297) Trinh, T. T.; Rozanska, X.; Delbecq, F.; Sautet, P., The Initial Step of Silicate versus Aluminosilicate Formation in Zeolite Synthesis: a Reaction Mechanism in Water with a Tetrapropylammonium Template, *Phys. Chem. Chem. Phys.* **2012**, *14*, 3369-3380.
(298) Rohling, R. Y.; Szyja, B. M.; Hensen, E. J. M., Insight into the Formation of Nanostructured MFI Sheets and MEL Needles Driven by Molecular Recognition, *J. Phys. Chem. C* **2019**, *123*, 5326-5335.
(299) Ciantar, M.; Mellot-Draznieks, C.; Nieto-Draghi, C., A Kinetic Monte Carlo Simulation Study of Synthesis Variables and Diffusion Coefficients in Early Stages of Silicate Oligomerization, *J. Phys. Chem. C* **2015**, *119*, 28871-28884.
(300) Bertoncini, F.; Bonduelle-Skrzypcak, A.; Francis, J.; Guillon, E.,Hydrocracking, In *Catalysis by transition metal sulphides: from molecular theory to industrial applications*; Toulhoat, H., Raybaud, P., Eds.; Editions Technip: 2013, p 609-677.
(301) Huber, G. W.; Cortright, R. D.; Dumesic, J. A., Renewable Alkanes by Aqueous-Phase Reforming of Biomass-Derived Oxygenates, *Angew. Chem. Int. Ed.* **2004**, *43*, 1549-1551.
(302) Bond, J. Q.; Alonso, D. M.; Wang, D.; West, R. W.; Dumesic, J. A., Integrated Catalytic Conversion of g-Valerolactone to Liquid Alkenes for Transportation Fuels, *Science* **2010**, *327*, 1110-1114.
(303) Hahn, M. W.; Copeland, J. R.; van Pelt, A. H.; Sievers, C., Stability of Amorphous Silica-Alumina in Hot Liquid Water, *ChemSusChem* **2013**, *6*, 2304-2315.
(304) Larmier, K.; Chizallet, C.; Maury, S.; Cadran, N.; Abboud, J.; Lamic-Humblot, A. F.; Marceau, E.; Lauron-Pernot, H., Isopropanol Dehydration on Amorphous Silica-Alumina: Synergy of Bronsted and Lewis Acidities at Pseudo-Bridging Silanols, *Angew. Chem. Int. Ed.* **2017**, *56*, 230-234.
(305) Wang, Z.; Li, T.; Jiang, Y.; Lafon, O.; Liu, Z.; Trebosc, J.; Baiker, A.; Amoureux, J. P.; Huang, J., Acidity Enhancement Through Synergy of Penta- and Tetra-Coordinated Aluminum Species in Amorphous Silica Networks, *Nature Commun.* **2020**, *11*, 225.
(306) Zirl, D. M.; Garofalini, S. H., Structure of Sodium Aluminosilicate Glasses, *J. Am. Ceram. Soc.* **1990**, *73*, 2848-2856.
(307) Charpentier, T.; Menziani, M. C.; Pedone, A., Computational Simulations of Solid State NMR Spectra: a New Era in Structure Determination of Oxide Glasses, *RSC Advances* **2013**, *3*, 10550.
(308) Benoit, M.; Ispas, S.; Tuckerman, M., Structural Properties of Molten Silicates from Ab Initio Molecular-Dynamics Simulations: Comparison Between CaO-Al_2O_3-SiO_2 and SiO_2, *Phys. Rev. B* **2001**, *64*, 224205.
(309) Dongol, R.; Wang, L.; Cormack, A. N.; Sundaram, S. K., Molecular Dynamics Simulation of Sodium Aluminosilicate Glass Structures and Glass Surface-Water Reactions Using the Reactive Force Field (ReaxFF), *Appl. Surf. Sci.* **2018**, *439*, 1103-1110.
(310) Bauchy, M., Deciphering the Atomic Genome of Glasses by Topological Constraint Theory and Molecular Dynamics: A Review, *Comput. Mater. Sci.* **2019**, *159*, 95-102.
(311) Chizallet, C.; Raybaud, P., Acidity of Amorphous Silica–Alumina: From Coordination Promotion of Lewis Sites to Proton Transfer, *ChemPhysChem* **2010**, *11*, 105-108.
(312) Katada, N.; Niwa, M., Silica Monolayer Solid-Acid Catalyst Prepared by CVD, *Chem. Vap. Deposition* **1996**, *2*, 125-134.

(313) Sarrazin, P.; Kasztelan, S.; Zanier-Szydlowski, N.; Bonnelle, J. P.; Grimblot, J., Interaction of Oxomolybdenum Species with g-Al_2O_3 and g-Al_2O_3 Modified by Silicon. 1. The SiO_2/g-Al_2O_3 System, *J. Phys. Chem.* **1993**, *97*, 5947-5953.
(314) Caillot, M.; Chaumonnot, A.; Digne, M.; Poleunis, C.; Debecker, D. P.; van Bokhoven, J. A., Synthesis of Amorphous Aluminosilicates by Grafting: Tuning the Building and Final Structure of the Deposit by Selecting the Appropriate Synthesis Conditions, *Microporous Mesoporous Mater.* **2014**, *185*, 179-189.
(315) Digne, M.; Sautet, P.; Raybaud, P.; Euzen, P.; Toulhoat, H., Hydroxyl Groups on Gamma-Alumina Surfaces: a DFT Study, *J. Catal.* **2002**, *211*, 1-5.
(316) Digne, M.; Sautet, P.; Raybaud, P.; Euzen, P.; Toulhoat, H., Use of DFT to Achieve a Rational Understanding of Acid–Basic Properties of Gamma-Alumina Surfaces, *J. Catal.* **2004**, *226*, 54-68.
(317) De Witte, B. M.; Grobet, P. J.; Uytterhoeven, J. B., Pentacoordinated Aluminum in Noncalcined Amorphous Aluminosilicates, Prepared in Alkaline and Acid Medium, *J. Phys. Chem.* **1995**, *99*, 6961-6965.
(318) Gilson, J. P.; Edwards, G. C.; Peters, A. W.; Rajagopalan, K.; Wormsbecher, R. F.; Roberie, T. G.; Shatlock, M. P., Penta-Coordinated Aluminium in Zeolites and Aluminosilicates, *J. Chem. Soc., Chem. Commun.* **1987**, 91-92.
(319) Sandupatla, A. S.; Alexopoulos, K.; Reyniers, M.-F.; Marin, G. B., DFT Investigation into Alumina ALD Growth Inhibition on Hydroxylated Amorphous Silica Surface, *J. Phys. Chem. C* **2015**, *119*, 18380-18388.
(320) Handzlik, J.; Grybos, R.; Tielens, F., Isolated Chromium(VI) Oxide Species Supported on Al-Modified Silica: A Molecular Description, *J. Phys. Chem. C* **2016**, *120*, 17594–17603.
(321) Perez-Beltran, S.; Balbuena, P. B.; Ramírez-Caballero, G. E., Surface Structure and Acidity Properties of Mesoporous Silica SBA-15 Modified with Aluminum and Titanium: First-Principles Calculations, *J. Phys. Chem. C* **2016**, *120*, 18105-18114.
(322) Moses, A. W.; Ramsahye, N. A.; Raab, C.; Leifeste, H. D.; Chattopadhyay, S.; Chmelka, B. F.; Eckert, J.; Scott, S. L., Methyltrioxorhenium Interactions with Lewis Acid Sites of an Amorphous Silica-Alumina, *Organometallics* **2006**, *25*, 2157-2165.
(323) Duchateau, R.; Harmsen, R. J.; Abbenhuis, H. C. L.; van Santen, R.; Meetsma, A.; Thiele, S. K. H.; Kranenburg, M., Modeling Acidic Sites in Zeolites and Aluminosilicates by Aluminosilsesquioxanes, *Chem. Eur. J.* **1999**, *5*, 3130-3135.
(324) Shyam Lokare, K.; Frank, N.; Braun-Cula, B.; Goikoetxea, I.; Sauer, J.; Limberg, C., Trapping Aluminum Hydroxide Clusters with Trisilanols during Speciation in Aluminum(III)–Water Systems:Reproducible,Large Scale Access to Molecular Aluminate Models, *Angew. Chem., Int. Ed* **2016**, *55*, 12325-12329.
(325) Lokare, K. S.; Braun-Cula, B.; Limberg, C.; Jorewitz, M.; Kelly, J. T.; Asmis, K. R.; Leach, S.; Baldauf, C.; Goikoetxea, I.; Sauer, J., Structure and Reactivity of Al-O(H)-Al Moieties in Siloxide Frameworks: Solution and Gas-Phase Model Studies, *Angew. Chem. Int. Edit.* **2019**, *58*, 902-906.
(326) Tielens, F.; Gervais, C.; Lambert, J. F.; Mauri, F.; Costa, D., Ab Initio Study of the Hydroxylated Surface of Amorphous Silica: A Representative Model, *Chem. Mater.* **2008**, *20*, 3336-3344.
(327) Lippmaa, E.; Magi, M.; Samoson, A.; Tarmak, M.; Engelhardt, G., Investigation of the Structure of Zeolites by Solid-state High-Resolution ^{29}Si NMR Spectroscopy, *J. Am. Chem. Soc.* **1981**, *103*, 4992-4996.
(328) Lippmaa, E.; Samoson, A.; Engelhardt, G.; Grimmer, A. R., Structural Studies of Silicates by Solid-State High-Resolution ^{29}Si NMR, *J. Am. Chem. Soc.* **1980**, *102*, 4889-4893.
(329) Murdoch, J. B.; Stebbins, J. F.; Carmichael, I. E. S., High-Resolution ^{29}Si NMR Study of Silicate and Aluminosilicate Glasses: the Effect of Network-Modifying Cations, *Am. Mineral.* **1985**, *70*, 332-343.
(330) Maciel, G. E.; Sindorf, D. W., Silicon-29 NMR Study of the Surface of Silica Gel by Cross Polarization and Magic-Angle Spinning, *J. Am. Chem. Soc.* **1980**, *102*, 7606-7607.
(331) Sato, S.; Sodesawa, T.; Nozaki, F., Solid-State NMR of Silica-Alumina Prepared by CVD, *J. Mol. Catal.* **1991**, *66*, 343-355.

(332) Pauling, L. *The nature of the chemical bond and the structure of molecules and crystals : an introduction to modern structural chemistry*; Cornell University Press: London, 1960.
(333) Chizallet, C.; Digne, M.; Arrouvel, C.; Raybaud, P.; Delbecq, F.; Costentin, G.; Che, M.; Sautet, P.; Toulhoat, H., Insights into the Geometry, Stability and Vibrational Properties of OH Groups on g-Al_2O_3, TiO_2-Anatase and MgO from DFT Calculations, *Topics Catal.* **2009**, *52*, 1005-1016.
(334) Busca, G., Catalytic Materials Based on Silica and Alumina: Structural Features and Generation of Surface Acidity, *Prog. Mater. Sci.* **2019**, *104*, 215-249.
(335) Bevilacqua, M.; Montanari, T.; Finocchio, E.; Busca, G., Are the Active Sites of Protonic Zeolites Generated by the Cavities?, *Catal. Today* **2006**, *116*, 132-142.
(336) Garrone, E.; Onida, B.; Bonelli, B.; Busco, C.; Ugliengo, P., Molecular Water on Exposed Al^{3+} Cations Is a Source of Acidity in Silicoaluminas, *J. Phys. Chem. B* **2006**, *110*, 19087-19092.
(337) Blanchard, J.; Krafft, J.-M.; Dupont, C.; Sayag, C.; Takahashi, T.; Yasuda, H., On the Influence of Water Traces on the Acidity Measurement of Amorphous Aluminosilicates, *Catal. Today* **2014**, *226*, 89-96.
(338) Phung, T. K.; Busca, G., Diethyl Ether Cracking and Ethanol Dehydration: Acid Catalysis and Reaction Paths, *Chem. Eng. J.* **2015**, *272*, 92-101.
(339) Larmier, K.; Chizallet, C.; Cadran, N.; Maury, S.; Abboud, J.; Lamic-Humblot, A.-F.; Marceau, E.; Lauron-Pernot, H., Mechanistic Investigation of Isopropanol Conversion on Alumina Catalysts: Location of Active Sites for Alkene/Ether Production, *ACS Catal.* **2015**, *5*, 4423-4437.
(340) Larmier, K.; Nicolle, A.; Chizallet, C.; Cadran, N.; Maury, S.; Lamic-Humblot, A.-F.; Marceau, E.; Lauron-Pernot, H., Influence of Coadsorbed Water and Alcohol Molecules on Isopropyl Alcohol Dehydration on γ-Alumina: Multiscale Modeling of Experimental Kinetic Profile, *ACS Catal.* **2016**, *6*, 1905-1920.
(341) Makarova, M. A.; Williams, C.; Zamaraev, K. I.; Thomas, J. M., Mechanistic Study of Sec-Butyl Alcohol Dehydration on Zeolite H-ZSM-5 and Amorphous Aluminosilicate, *J. Chem. Soc., Faraday Trans.* **1994**, *90*, 2147-2153.
(342) Makarova, M. A.; Paukshtis, E. A.; Thomas, J. M.; Williams, C.; Zamaraev, K. I., Dehydration of n-Butanol on Zeolite H-ZSM-5 and Amorphous Aluminosilicate: Detailed Mechanistic Study and the Effect of Pore Confinement, *J. Catal.* **1994**, *149*, 36-51.
(343) Phung, T. K.; Proietti Hernández, L.; Lagazzo, A.; Busca, G., Dehydration of Ethanol over Zeolites, Silica Alumina and Alumina: Lewis Acidity, Brønsted Acidity and Confinement Effects, *Appl. Catal. A* **2015**, *493*, 77-89.
(344) Weitkamp, J., Catalytic Hydrocracking—Mechanisms and Versatility of the Process, *ChemCatChem* **2012**, *4*, 292-306.
(345) Bouchy, C.; Hastoy, G.; Guillon, E.; Martens, J. A., Fischer-Tropsch Waxes Upgrading via Hydrocracking and Selective Hydroisomerization, *Oil Gas Sci. Technol. - Rev. IFP* **2009**, *64*, 91-112.
(346) Zečević, J.; van der Eerden, A. M. J.; Friedrich, H.; de Jongh, P. E.; de Jong, K. P., Heterogeneities of the Nanostructure of Platinum/Zeolite Y Catalysts Revealed by Electron Tomography, *ACS Nano* **2013**, *7*, 3698-3705.
(347) Zecevic, J.; Vanbutsele, G.; de Jong, K. P.; Martens, J. A., Nanoscale Intimacy in Bifunctional Catalysts for Selective Conversion of Hydrocarbons, *Nature* **2015**, *528*, 245-248.
(348) Gutierrez-Acebo, E.; Leroux, C.; Chizallet, C.; Schuurman, Y.; Bouchy, C., Metal/Acid Bifunctional Catalysis and Intimacy Criterion for Ethylcyclohexane Hydroconversion: When Proximity Does Not Matter, *ACS Catal.* **2018**, *8*, 6035-6046.
(349) Weisz, P. B., Polyfunctional Heterogeneous Catalysis, *Adv. Catal.* **1962**, *13*, 137-190.
(350) Markova, V. K.; Vayssilov, G. N.; Genest, A.; Rosch, N., Adsorption and Transformations of Ethene on Hydrogenated Rhodium Clusters in Faujasite-Type Zeolite. A Computational Study, *Catal. Sci. Technol.* **2016**, *6*, 1726-1736.
(351) Grybos, R.; Benco, L.; Bucko, T.; Hafner, J., Molecular Adsorption and Metal-Support Interaction for Transition-Metal Clusters in Zeolites: NO Adsorption on Pd_n (n=1–6) Clusters in Mordenite, *J. Chem. Phys.* **2009**, *130*, 104503:104501-104520.
(352) Joshi, A. M.; Delgass, W. N.; Thomson, K. T., Adsorption of Small Au_n (n = 1−5) and Au−Pd Clusters Inside the TS-1 and S-1 Pores, *J. Phys. Chem. B* **2006**, *110*, 16439-16451.

(353) Moc, J.; Musaev, D. G.; Morokuma, K., Zeolite-Supported Palladium Tetramer and Its Reactivity toward H_2 Molecules: Computational Studies, *J. Phys. Chem. A* **2008**, *112*, 5973-5983.
(354) Mikhailov, M. N.; Kustov, L. M.; Kazansky, V. B., The State and Reactivity of Pt_6 Particles in ZSM-5 Zeolite, *Catal. Lett.* **2007**, *120*, 8-13.
(355) Mikhailov, M. N.; Mishin, I. V.; Kustov, L. M.; Mordkovich, V. Z., The Structure and Activity of Pt_6 particles in ZSM-5 Type Zeolites, *Catal. Today* **2009**, *144*, 273-277.
(356) Mikhailov, M. N.; Mishin, I. V.; Kustov, L. M., Platinum Nanoparticles as Active Sites for C–C Bond Activation in High-Silica Zeolites, *Microporous Mesoporous Mater.* **2009**, *117*, 603-608.
(357) Petkov, P. S.; Petrova, G. P.; Vayssilov, G. N.; Rösch, N., Saturation of Small Supported Metal Clusters by Adsorbed Hydrogen. A Computational Study on Tetrahedral Models of Rh_4, Ir_4, and Pt_4, *J. Phys. Chem. C* **2010**, *114*, 8500-8506.
(358) Vayssilov, G. N.; Rösch, N., Reverse Hydrogen Spillover in Supported Subnanosize Clusters of the Metals of Groups 8 to 11. A Computational Model Study, *Phys. Chem. Chem. Phys.* **2005**, *7*, 4019-4026.
(359) Hu, C. H.; Chizallet, C.; Mager-Maury, C.; Corral Valero, M.; Sautet, P.; Toulhoat, H.; Raybaud, P., Modulation of Catalyst Particle Structure upon Support Hydroxylation: *Ab Initio* Insights for Pd_{13} and Pt_{13} / Gamma-Al_2O_3, *J. Catal.* **2010**, *274*, 99-110.
(360) Mager-Maury, C.; Bonnard, G.; Chizallet, C.; Sautet, P.; Raybaud, P., H_2-Induced Reconstruction of Supported Pt Clusters: Metal–Support Interaction *versus* Surface Hydride, *ChemCatChem* **2011**, *3*, 200-207.
(361) Jahel, A.; Moizan-Baslé, V.; Chizallet, C.; Raybaud, P.; Olivier-Fourcade, J.; Jumas, J. C.; Avenier, P.; Lacombe, S., Effect of Indium-Doping of Gamma-Alumina on the Stabilization of PtSn Alloy Clusters Prepared by Surface Organostannic Chemistry, *J. Phys. Chem. C* **2012**, *116*, 10073-10083.
(362) Mager-Maury, C.; Chizallet, C.; Sautet, P.; Raybaud, P., Platinum Nano-Clusters Stabilized on g-alumina by Chlorine Used as a Capping Surface Ligand: a DFT Study, *ACS Catal.* **2012**, *2*, 1346-1357.
(363) Gorczyca, A.; Moizan, V.; Chizallet, C.; Proux, O.; Del Net, W.; Lahera, E.; Hazemann, J. L.; Raybaud, P.; Joly, Y., Monitoring Morphology and Hydrogen Coverage of Nanometric Pt/Gamma-Al_2O_3 Particles by *in situ* HERFD–XANES and Quantum Simulations, *Angew. Chem., Int. Ed.* **2014**, *53*, 12426 –12429.
(364) Gorczyca, A.; Raybaud, P.; Moizan, V.; Joly, Y.; Chizallet, C., Atomistic Models for Highly-Dispersed PtSn/γ-Al_2O_3 Catalysts: Ductility and Dilution Affect the Affinity for Hydrogen, *ChemCatChem* **2019**, *11*, 3941–3951.
(365) Raybaud, P.; Chizallet, C.; Mager-Maury, C.; Digne, M.; Toulhoat, H.; Sautet, P., From Gamma-Alumina to Supported Platinum Nanoclusters in Reforming Conditions: 10 years of DFT Modeling and Beyond, *J. Catal.* **2013**, *308*, 328-340.
(366) Zhao, W.; Chizallet, C.; Sautet, P.; Raybaud, P., Dehydrogenation Mechanisms of Methyl-Cyclohexane on γ-Al_2O_3 Supported Pt_{13}: Impact of Cluster Ductility, *J. Catal.* **2019**, *370*, 118-129.